Finding regulatory modules of chemical reaction systems

Yuhei Yamauchi [1,*] Atsuki Hishida,[2] Takashi Okada [1] and Atsushi Mochizuki[1]
[1]*Institute for Life and Medical Sciences, Kyoto University, Kyoto 606-8507, Japan*
[2]*Graduate School of Science, Kyoto University, Kyoto 606-8502, Japan*

(Received 23 October 2023; accepted 9 April 2024; published 10 May 2024)

Within a cell, numerous chemical reactions form chemical reaction networks (CRNs), which are the origins of cellular functions. We previously developed a theoretical method called structural sensitivity analysis (SSA), which enables us to determine, solely from the network structure, the qualitative changes in the steady-state concentrations of chemicals resulting from the perturbations to a parameter. Notably, if a subnetwork satisfies specific topological conditions, it is referred to as a buffering structure, and the effects of perturbations to the parameter within the subnetwork are localized to the subnetwork (the law of localization). A buffering structure can be the origin of modularity in the regulation of cellular functions generated from CRNs. However, an efficient method to search for buffering structures in a large CRN has not yet been established. In this study, we prove the "inverse theorem" of the law of localization, which states that a certain subnetwork exhibiting a confined response range is always a buffering structure. In other words, we are able to identify buffering structures in terms of confined responses rather than the topological conditions. By leveraging this property, we develop an algorithm to enumerate all buffering structures for a given network by calculating responses. Additionally, we show that the hierarchy of perturbed response patterns corresponds to that of buffering structures, and present a method to illustrate the hierarchy. Our method will be a powerful tool for understanding the regulation of cellular functions generated from CRNs.

DOI: 10.1103/PhysRevResearch.6.023150

I. INTRODUCTION

In living cells, chemical reactions are connected by sharing their products and substrates, forming chemical reaction networks (CRNs), such as metabolic networks and signal transduction networks. The dynamical behavior of chemicals derived from these CRNs underlies physiological functions, such as metabolism, cell cycle control, and signal transduction. Each reaction is regulated by enzyme activity, and changes in enzyme activity cause dynamical changes in the concentration of each chemical in the system. It is widely believed that cells regulate physiological functions through the modulation of enzyme activity [1–7]. Various physiological functions can arise even from a single CRN. For instance, a metabolic network is composed of many subcircuits, such as carbon metabolism and the amino acid synthesis pathway [8]. Since different subcircuits can share the same chemicals, these subcircuits are interconnected with each other, forming a single connected metabolic network [9–11]. It is unclear how different subcircuits are regulated separately because the modulation of one subcircuit can affect other subcircuits.

We previously developed a theoretical framework that may provide an answer to this question [12,13]. This is based on structural sensitivity analysis (SSA) [14], which allows us to determine, solely from the structure of a CRN, the qualitative changes (no change, increase, or decrease) in steady-state concentrations of each chemical in response to the modulation of enzyme activity (sensitivities). In SSA, the parameters are either the activities of the enzymes catalyzing the reactions (reaction rate parameters) or the conserved quantities. The concept of "buffering structures" derived from SSA is important for understanding the range within which the effects of changes in parameters propagate within a CRN in terms of network topology [12,13]. A subnetwork in a CRN, consisting of a subset of chemicals and a subset of reactions, is called a buffering structure when it satisfies the following two conditions: (i) The subnetwork contains all reactions whose reaction rates depend on the concentrations of chemicals within it ("output-complete"). (ii) The index, defined by the −(the number of chemicals)+(the number of reactions)−(the number of cycles) is equal to zero. It has been mathematically demonstrated that the steady-state responses to the perturbation of a parameter within a buffering structure are confined within the buffering structure. When distinct nonoverlapping buffering structures (denoted by Γ_1 and Γ_2) coexist within a network, the perturbations to parameters within Γ_1 do not affect the steady-state concentration of chemicals within Γ_2, and vice versa. In this sense, independent regulation between distinct buffering structures is achieved. Taking biological networks for example, the tricarboxylic acid (TCA) cycle and the pentose phosphate pathway (PPP) in metabolic networks are

*yamauchi.yuhei.8c@kyoto-u.ac.jp

contained in separate buffering structures [12], indicating that it is possible to modulate the TCA cycle without affecting the PPP pathway, and vice versa. A buffering structure represents a novel concept in CRNs: a "regulatory module" can naturally arise from network topology. Finding all the buffering structures in a given CRN will be important for clarifying how different functions arising from a CRN are regulated.

In Ref. [12], it is pointed out that the existence of buffering structures can provide the system with a property called "perfect adaptation". A system is said to exhibit adaptation if it shows a transient response to a stimulus and goes back to the original state [15–18]. A well-known example is the response of bacteria to changes in the nutrient concentration during chemotaxis [19–21]. In particular, if, after a perturbation to a parameter, the system eventually returns to its original state exactly, it is called perfect adaptation, which has been studied theoretically [22].

While exploring the buffering structures in a CRN is important, an efficient method to search for all of them has not been established. One approach to search for buffering structures is to check, for all subnetworks of CRNs, if the aforementioned two conditions are satisfied (the "brute-force method"). However, as the size of the CRN increases, the number of candidate subnetworks grows significantly, leading to a substantial increase in the computational cost. In previous studies [12,13,23], an *ad hoc* method was employed where buffering structures are identified by searching for candidate subnetworks that show confined responses, using the calculation of sensitivities. However, it remained unclear whether all subnetworks calculated from the method satisfy the topological conditions of buffering structures.

In this study, we prove the "inverse theorem" of the law of localization, which states that an output-complete subnetwork exhibiting a confined response range ("regulatory module") is always a buffering structure. This ensures that buffering structures can be exhaustively identified by all of the regulatory modules, which are obtained via the sensitivity calculation. The proposed method is much more efficient than the brute-force method. We implemented the algorithm as Python pipelines, called ibuffpy [48].

The terms "network modules" or "regulatory modules" have been used in the study of biological networks [24–27], yet their definitions are vague and unclear. For instance, Ref. [24] studied the statistical properties of graph structures, defined network modules based on the clustering coefficients of CRNs in databases. Nonetheless, the biological functions of such network modules remain unclear. Here, we define a subnetwork with a confined response property as a regulatory module. We show that such a subnetwork always satisfies certain topological conditions. In other words, we determine the necessary and sufficient conditions for a subnetwork to be a regulatory module. This enables us to discuss the emergence of the biological function of a regulatory module directly from network topology.

We previously found that the nonzero response patterns under perturbations of different parameters can exhibit inclusion relations among them, i.e., they exhibit hierarchical structures [12]. In addition, buffering structures have been suggested to exhibit inclusion relations [12]. Based on the inverse theorem, we show that a buffering structure and a confined response have a one-to-one correspondence. We thus understand that nonzero response patterns always show hierarchical patterns. Furthermore, we propose an algorithm to depict this hierarchy graphically through the computation of buffering structures, which is also implemented in ibuffpy.

The paper is organized as follows. In Sec. II, we briefly review SSA and the concept of a buffering structure presented in Refs. [12,14]. In Sec. III, we prove our main theorem: the inverse theorem of the law of localization. In Sec. IV, we present an efficient algorithm to exhaustively find buffering structures. In Sec. V, we show the equivalence between the hierarchy of nonzero responses and that of buffering structures. We also propose an algorithm to depict the hierarchy graph. In the main text, we assume that CRNs do not have conserved quantities, but our results can be generalized to CRNs with conserved quantities, as discussed in Appendix A.

II. THE SETTING AND REVIEW OF STRUCTURAL SENSITIVITY ANALYSIS

A. Setting

We label chemicals by m ($m = 1, \dots, M$) and reactions by n ($n = 1, \dots, N$), and consider a spatially homogeneous CRN [12,14,28–32] consisting of the following reactions:

$$y_{1,n}X_1 + \cdots + y_{M,n}X_M \to y'_{1,n}X_1 + \cdots + y'_{M,n}X_M, \quad n = 1, \dots, N. \tag{1}$$

A state of the reaction system, specified by concentrations $x_m(t)$, obeys the differential equations

$$\frac{dx_m(t)}{dt} = \sum_{n=1}^{N}(y'_{m,n} - y_{m,n})r_n(t) = \sum_{n=1}^{N}\nu_{m,n}r_n(t). \tag{2}$$

Here, the $M \times N$ matrix $\boldsymbol{\nu}$ is called the stoichiometric matrix, defined as $\nu_{m,n} \coloneqq y'_{m,n} - y_{m,n}$. $r_n(t)$ is the reaction rate (flux) of the reaction n. With $\boldsymbol{x}(t) \coloneqq (x_1(t), \dots, x_M(t))^\top$, $\boldsymbol{r}(t) \coloneqq (r_1(t), \dots, r_N(t))^\top$, Eq. (2) can be written as

$$\frac{d\boldsymbol{x}(t)}{dt} = \boldsymbol{\nu}\boldsymbol{r}(t). \tag{3}$$

We assume that the flux function r_n depends on its reaction rate parameter k_n, i.e.,

$$\frac{\partial r_n}{\partial k_n} \neq 0. \tag{4}$$

In metabolic networks, k_n can be the activity or the amount of the enzyme catalyzing the reaction n. In addition, we assume that each flux function r_n is strictly increasing with respect to the concentrations of its substrates. We also account for regulations such as allosteric effects,

$$\begin{aligned}
&\frac{\partial r_n}{\partial x_m} > 0, \quad \text{if} \quad y_{m,n} > 0 \quad or \quad m \in \mathcal{M}_n^+, \\
&\frac{\partial r_n}{\partial x_m} < 0, \quad \text{if} \quad m \in \mathcal{M}_n^-, \\
&\frac{\partial r_n}{\partial x_m} = 0, \quad \text{otherwise},
\end{aligned} \tag{5}$$

where $\mathcal{M}_n^+$ and $\mathcal{M}_n^-$ are the set of chemicals that are not a substrate of the reaction n but regulate the reaction positively and negatively, respectively. Popular kinetics, such as the mass action ($r_n = k_n \prod_{m=1}^{M} x_m^{y_{m,n}}$) and the Michaelis-Menten kinetics, satisfy this condition. In the following, we do not assume specific forms of r_n except for the assumptions in Eqs. (4) and (5).

B. Structural sensitivity analysis

We briefly review the structural sensitivity analysis [12–14]. This analysis allows us to determine qualitative changes in the steady-state concentration of each chemical x_m in response to changes in a reaction rate parameter k_n (sensitivities).

We assume that the system has a steady state $\boldsymbol{x}$. At the steady state, the steady-state flux vector $\boldsymbol{r}$ satisfies $\boldsymbol{\nu r} = \boldsymbol{0}$, i.e., $\boldsymbol{r} \in \ker \boldsymbol{\nu}$. We choose a basis for $\ker \boldsymbol{\nu}$ as $\{\boldsymbol{c}_i\}_{i=1}^K$ ($K := \dim \ker \boldsymbol{\nu}$). $\boldsymbol{r}$ can be written as a linear combination of $\{\boldsymbol{c}_i\}_{i=1}^K$,

$$\boldsymbol{r} = \mu_1 \boldsymbol{c}_1 + \cdots + \mu_K \boldsymbol{c}_K, \tag{6}$$

where $\mu_1, \ldots, \mu_K \in \mathbb{R}$. Under the perturbation of $k_n \to k_n + \delta k_n$, each flux changes from r_j to $r_j + \delta r_j$. δr_j can be written as

$$\delta r_j = \delta k_n \sum_{p=1}^{K} \frac{\partial \mu_p}{\partial k_n} c_{p,j}, \tag{7}$$

where $c_{p,j}$ is the jth component of $\boldsymbol{c}_p$.

At the same time, the total derivative of r_j is given by

$$\delta r_j = \delta k_n \left\{ \delta_{n,j} \frac{\partial r_j}{\partial k_n} + \sum_{m=1}^{M} r_{j,m} \frac{\partial x_m}{\partial k_n} \right\}, \tag{8}$$

where $\delta_{n,j}$ is a Kronecker delta and $r_{j,m} := \frac{\partial r_j}{\partial x_m}$.

From Eqs. (7) and (8),

$$\sum_{m=1}^{M} r_{j,m} \frac{\partial x_m}{\partial k_n} - \sum_{p=1}^{K} \frac{\partial \mu_p}{\partial k_n} c_{p,j} = -\delta_{n,j} \frac{\partial r_j}{\partial k_n}. \tag{9}$$

Let us define the matrices $\boldsymbol{A} \in \mathbb{R}^{N \times (M+K)}$ and $\tilde{\boldsymbol{S}} \in \mathbb{R}^{(M+K) \times N}$ at the steady state as follows:

$$\boldsymbol{A} := \left(\begin{array}{ccc|ccc} r_{1,1} & \cdots & r_{1,M} & & & \\ \vdots & & \vdots & -\boldsymbol{c}_1 & \cdots & -\boldsymbol{c}_K \\ r_{N,1} & \cdots & r_{N,M} & & & \end{array} \right), \tag{10}$$

$$\tilde{\boldsymbol{S}} := \left(\begin{array}{ccc} \frac{\partial x_1}{\partial k_1} & \cdots & \frac{\partial x_1}{\partial k_N} \\ \vdots & & \vdots \\ \frac{\partial x_M}{\partial k_1} & \cdots & \frac{\partial x_M}{\partial k_N} \\ \hline \frac{\partial \mu_1}{\partial k_1} & \cdots & \frac{\partial \mu_1}{\partial k_N} \\ \vdots & & \vdots \\ \frac{\partial \mu_K}{\partial k_1} & \cdots & \frac{\partial \mu_K}{\partial k_N} \end{array} \right). \tag{11}$$

All entries of these matrices are partial derivatives evaluated at the steady state. The upper part of $\tilde{\boldsymbol{S}}$ represents the rate of change in the steady-state concentration of each chemical with respect to each reaction rate parameter. The lower part of $\tilde{\boldsymbol{S}}$ reflects the rate of change in the steady-state flux, which is given by Eq. (7).

From Eq. (9), we obtain

$$\boldsymbol{A}\tilde{\boldsymbol{S}} = -\begin{pmatrix} \frac{\partial r_1}{\partial k_1} & \cdots & 0 \\ \vdots & \ddots & \vdots \\ 0 & \cdots & \frac{\partial r_N}{\partial k_N} \end{pmatrix}. \tag{12}$$

To present the key idea, we assume that $\boldsymbol{A}$ and $\tilde{\boldsymbol{S}}$ are square matrices, i.e., $M + K = N$. In this case, $\dim \ker \boldsymbol{\nu}^\top = 0$ holds, implying that there are no conserved quantities in the system (see Appendix A for the general case). With Eq. (4) in mind, we obtain the following result.

Theorem 1. [14] If $\boldsymbol{A}$ is invertible,

$$\tilde{\boldsymbol{S}} \propto -\boldsymbol{A}^{-1} := \boldsymbol{S}. \tag{13}$$

Here, $\boldsymbol{X} \propto \boldsymbol{Y}$ means the algebraic distribution of zero entries of matrices $\boldsymbol{X}$ and $\boldsymbol{Y}$ are the same. Using Eq. (5), the distribution of zero entries of $\boldsymbol{A}$ is algebraically determined from the network structure, so is that of $\tilde{\boldsymbol{S}}$. If $S_{m,n} = 0$ holds algebraically, the perturbation of k_n never affects the steady-state concentration of the chemical m, regardless of the values of $r_{j,m}$ ($\neq 0$), in which case we say "the reaction n does not influence the chemical m". If $S_{m,n} \neq 0$ algebraically, there can exist some parameters or kinetics such that the perturbation of k_n affects the steady-state concentration of the chemical m, in which case we say "the reaction n influences the chemical m". Overall, qualitative changes in the steady-state concentrations of chemicals in response to perturbation to each reaction rate parameter can be determined solely from the topology of a CRN. Note that if $\frac{\partial r_n}{\partial k_n} > 0$ holds for $n = 1, \ldots, N$, the signs of each entry in $\tilde{\boldsymbol{S}}$ and those in $\boldsymbol{S}$ coincide, indicating that the signs of changes in the steady-state concentrations of each chemical can also be determined from network topology.

Remark 1. $\boldsymbol{A}$ and $\boldsymbol{S}$ depend on the choice of the basis for $\ker \boldsymbol{\nu}$. However, the sensitivity of the concentration of each chemical and flux at the steady state with respect to each reaction rate parameter k_n is independent of the choice of the basis, which we will prove in Lemma 1 (Sec. III).

Definition 1. (Regularity of a CRN). A CRN is called regular if it admits a steady state and the associated $\boldsymbol{A}$ is invertible.

We assume the regularity so that $\boldsymbol{A}$ is invertible throughout the paper.

C. Buffering structure

The concept of buffering structures derived from SSA is important for understanding, in terms of network topology, the extent to which the effects of changes in parameters propagate within a CRN [12,13]. When a subnetwork of a regular CRN satisfies certain topological conditions, the subnetwork is called a buffering structure (as defined in Definition 2). It was mathematically demonstrated that the steady-state responses to the perturbation of a parameter within a buffering structure are confined within the buffering structure (as shown in Theorem 2, the law of localization). We briefly review the law of localization and buffering structure [12]. Here, we consider CRNs that lack conserved quantities, that is, CRNs where $M + K = N$ holds. For the general case, see Appendix A.

Definition 2. (Buffering structure). [12] A subnetwork $\Gamma = (\mathfrak{m}_\Gamma, \mathfrak{r}_\Gamma)$ ($\mathfrak{m}_\Gamma$, $\mathfrak{r}_\Gamma$ are subsets of chemicals and reactions, respectively) of a regular CRN is a buffering structure if it satisfies:

(1) None of the reaction rates of the reactions in $\mathfrak{r}_\Gamma^c$ are dependent on the concentrations of chemicals within $\mathfrak{m}_\Gamma$, i.e., $\frac{\partial r_n}{\partial x_m}|_{\boldsymbol{x}} = 0$ at all $\boldsymbol{x}$, $\forall n \in \mathfrak{r}_\Gamma^c, \forall m \in \mathfrak{m}_\Gamma$, where $\mathfrak{r}_\Gamma^c$ means the complement of $\mathfrak{r}_\Gamma$ in all reactions in the CRN (output-complete),

(2) $\lambda(\Gamma) = 0$ with $\lambda(\Gamma) = -|\mathfrak{m}_\Gamma| + |\mathfrak{r}_\Gamma| - N(\mathfrak{r}_\Gamma)$.

Here, $|\mathfrak{m}_\Gamma|$ and $|\mathfrak{r}_\Gamma|$ are the size of $\mathfrak{m}_\Gamma$ and $\mathfrak{r}_\Gamma$, respectively, $N(\mathfrak{r}_\Gamma)$ is the number of stoichiometric cycles in $\mathfrak{r}_\Gamma$. To be precise, $N(\mathfrak{r}_\Gamma) \coloneqq \dim \{\boldsymbol{x} \in \ker \boldsymbol{v} \mid \mathrm{supp}\, \boldsymbol{x} \subset \mathfrak{r}_\Gamma\}$, where $\mathrm{supp}\, \boldsymbol{r} \coloneqq \{i \mid r_i \neq 0\}$ for $\boldsymbol{r} \in \mathbb{R}^N$. In the graphical representation of a CRN, if Γ is output-complete, no reaction arrows outside of Γ leave from the nodes (chemicals) inside Γ. It is important to note that the definition of a buffering structure does not depend on the choice of a basis for $\ker \boldsymbol{v}$.

Using Theorem 1 we can deduce Theorem 2, the proof of which was described in Ref. [12].

Theorem 2. (Law of localization). [12] The steady-state chemical concentrations and reaction fluxes outside of a buffering structure $\Gamma = (\mathfrak{m}_\Gamma, \mathfrak{r}_\Gamma)$ do not change under any perturbation of the reaction rate parameters in $\mathfrak{r}_\Gamma$.

Theorem 2 implies that when a subnetwork within a CRN satisfies certain topological conditions, the impact of a parameter perturbation within a buffering structure is restricted to that subnetwork. A buffering structure introduces a novel concept in CRNs: a "regulatory module" can naturally arise from the topology of a network.

We illustrate SSA and buffering structures in an example network.

Example 1. We consider a straight pathway, shown in Fig. 1(a). The stoichiometric matrix is given by

$$\boldsymbol{v} = \begin{pmatrix} 1 & -1 & 0 & 0 \\ 0 & 1 & -1 & 0 \\ 0 & 0 & 1 & -1 \end{pmatrix}. \tag{14}$$

$\boldsymbol{v}$ has a kernel vector $\boldsymbol{c} = (1, 1, 1, 1)^\top$. Since $M = 3$, $N = 4$, and $K = 1$, $M + K = N$ holds, implying that the CRN does not have the conserved quantities. The matrix $\mathbf{A}$ is

$$\mathbf{A} = \left(\begin{array}{cccc|c} 0 & 0 & 0 & -1 \\ r_{2,\mathrm{P}} & 0 & 0 & -1 \\ 0 & r_{3,\mathrm{Q}} & 0 & -1 \\ 0 & 0 & r_{4,\mathrm{R}} & -1 \end{array}\right), \tag{15}$$

and the sensitivity is determined as

$$\mathbf{S} = -\mathbf{A}^{-1} = \left(\begin{array}{cccc} \frac{1}{r_{2,\mathrm{P}}} & -\frac{1}{r_{2,\mathrm{P}}} & 0 & 0 \\ \frac{1}{r_{3,\mathrm{Q}}} & 0 & -\frac{1}{r_{3,\mathrm{Q}}} & 0 \\ \frac{1}{r_{4,\mathrm{R}}} & 0 & 0 & -\frac{1}{r_{4,\mathrm{R}}} \\ \hline 1 & 0 & 0 & 0 \end{array}\right). \tag{16}$$

Since $r_{2,P}, r_{3,Q}, r_{4,R} > 0$ from Eq. (5), the distribution of nonzero entries in $\mathbf{S}$ can be determined. If $\frac{\partial r_n}{\partial k_n} > 0$, $\forall n$, the signs of changes in each chemical are given by

$$\mathbf{S} = -\mathbf{A}^{-1} = \left(\begin{array}{cccc} + & - & 0 & 0 \\ + & 0 & - & 0 \\ + & 0 & 0 & - \\ \hline + & 0 & 0 & 0 \end{array}\right), \tag{17}$$

where $+$ and $-$ represent qualitative responses under perturbations associated with column indices. For example, from the second column, we can see that the increase in the reaction rate parameter of the reaction 2 results in a decrease in the steady-state concentration of the chemical P, but the steady-state concentrations of either Q or R are not affected [Figs. 1(a) and 1(b)]. The subnetwork $\Gamma = \{\{\mathrm{P}\}, \{2\}\}$ is a buffering structure, because Γ is output-complete and $\lambda(\Gamma) = -|\mathfrak{m}_\Gamma| + |\mathfrak{r}_\Gamma| - N(\mathfrak{r}_\Gamma) = -1 + 1 - 0 = 0$ [Fig. 1(a), red box]. This explains why the steady-state concentrations of Q and R are insensitive to the perturbation to the reaction 2.

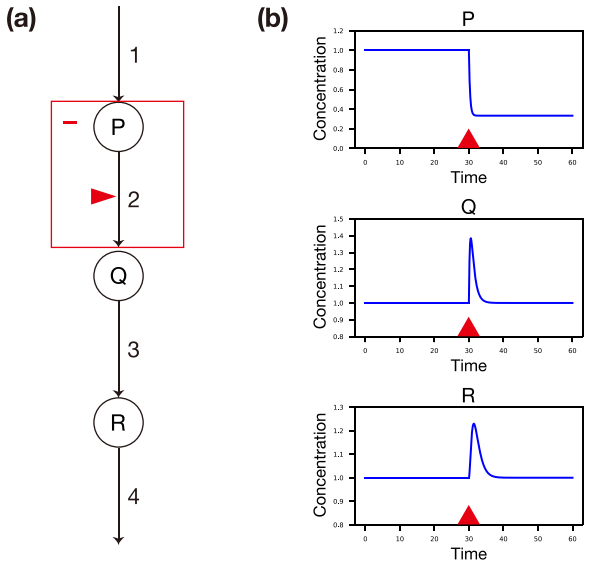

FIG. 1. Analysis for a hypothetical network (Example 1). (a) Graphical representation of a CRN comprising three chemicals (P, Q, R) and four reactions (1, 2, 3, 4). Solid lines indicate chemical reactions. The subnetwork $\Gamma = \{\{\mathrm{P}\}, \{2\}\}$ is a buffering structure. (b) The result of a numerical simulation in the network A. We assume $\boldsymbol{r} = (k_1, k_2 x_\mathrm{P}, k_3 x_\mathrm{Q}, k_4 x_\mathrm{R})$ with $(k_1, k_2, k_3, k_4) = (1.0, 1.0, 1.0, 1.0)$. The dynamics are in the steady state at $t = 30$. At $t = 30$, k_2 was increased by a factor of 2.

It was proved that the intersection or union of buffering structures is also a buffering structure [33].

Proposition 1. Let Γ_1 and Γ_2 be buffering structures of a regular CRN ($\Gamma_1 \neq \Gamma_2$). Then $\Gamma_1 \cup \Gamma_2$ and $\Gamma_1 \cap \Gamma_2$ are also buffering structures [33].

III. THE MAIN THEOREM

In this section, we present our main theorem: the inverse theorem of the law of localization. This theorem forms the basis for an efficient algorithm to identify buffering structures (Sec. IV). We first define a "regulatory module", which is an output-complete subnetwork with a confined response. As in the previous section, we consider CRNs that lack conserved

quantities, that is, CRNs where $M + K = N$ holds. For the general case, see Appendix A.

Definition 3. (Regulatory module). A subnetwork $\Psi = (\mathfrak{m}_\Psi, \mathfrak{r}_\Psi)$ ($\mathfrak{m}_\Gamma, \mathfrak{r}_\Psi$ are subsets of chemicals and reactions, respectively) of a regular CRN is a regulatory module if it satisfies

(1) Ψ is output-complete.

(2) The steady-state concentrations of $\mathfrak{m}^c_\Psi$ (chemicals outside of Ψ) do not change under the perturbation of either parameter in $\mathfrak{r}_\Psi$.

Remark 2. The condition 2 of Definition 3 does not require that the steady-state reaction fluxes outside of Ψ remain unchanged under perturbations of reaction rate parameters in Ψ. However, this can be easily derived from the requirements of Definition 3. Indeed, if a subnetwork $\Psi = (\mathfrak{m}_\Psi, \mathfrak{r}_\Psi)$ is a regulatory module, it is output-complete, which implies that reaction rates of $\mathfrak{r}^c_\Psi$ depend only on chemicals in $\mathfrak{m}^c_\Psi$. The steady-state concentrations of $\mathfrak{m}^c_\Psi$ do not change under either perturbations of reaction rate parameters in Ψ, therefore, steady-state reaction rates of $\mathfrak{r}^c_\Psi$ are not influenced by the perturbations.

From the law of localization (Theorem 2), a buffering structure is a regulatory module. We will prove the main theorem of this paper: The inverse theorem of the law of localization (Theorem 3), which states that a regulatory module is a buffering structure.

Theorem 3. (Inverse theorem of law of localization). Let Ψ be a regulatory module of a regular CRN. Then, Ψ is a buffering structure.

From Theorem 2 and Theorem 3, we obtain the following theorem.

Theorem 4. (The equivalence between a buffering structure and a regulatory module). Let Ψ be the subnetwork of a regular CRN. Then, the following are equivalent:

(i) Ψ is a buffering structure,

(ii) Ψ is a regulatory module.

To prove Theorem 3, we will prove two lemmas.

Lemma 1. The sensitivities of the steady-state concentration of each chemical and flux with respect to reaction parameters k_n are indifferent to the choices of a basis for $\ker \boldsymbol{\nu}$.

Proof of Lemma 1. Let $\{\boldsymbol{c}_i\}_{i=1,\dots,K}$ and $\{\boldsymbol{c}'_i\}_{i=1,\dots,K}$ be two distinct bases for $\ker \boldsymbol{\nu}$. We define $\boldsymbol{A}$ and $\boldsymbol{A}'$ as

$$\boldsymbol{A} := \left(\begin{array}{ccc|ccc} r_{1,1} & \dots & r_{1,M} & & & \\ \vdots & & \vdots & -\boldsymbol{c}_1 & \dots & -\boldsymbol{c}_K \\ r_{N,1} & \dots & r_{N,M} & & & \end{array}\right), \tag{18}$$

$$\boldsymbol{A}' := \left(\begin{array}{ccc|ccc} r_{1,1} & \dots & r_{1,M} & & & \\ \vdots & & \vdots & -\boldsymbol{c}'_1 & \dots & -\boldsymbol{c}'_K \\ r_{N,1} & \dots & r_{N,M} & & & \end{array}\right). \tag{19}$$

There exists an invertible change-of-basis matrix $\boldsymbol{P} \in \mathbb{R}^{K\times K}$ such that $\boldsymbol{c}'_i = p_{1,i}\boldsymbol{c}_1 + \cdots + p_{K,i}\boldsymbol{c}_K$ for $i = 1, \dots, K$. Using $\boldsymbol{P}$, we can rewrite $\boldsymbol{A}'$ as

$$\boldsymbol{A}' = \boldsymbol{A}\left(\begin{array}{c|c} \boldsymbol{I}_{M\times M} & \boldsymbol{0} \\ \hline \boldsymbol{0} & \boldsymbol{P} \end{array}\right). \tag{20}$$

From this equation, the sensitivity matrix $\boldsymbol{S}' := -(\boldsymbol{A}')^{-1}$ can be written in the form

$$\boldsymbol{S}' = \left(\begin{array}{c|c} \boldsymbol{I}_{M\times M} & \boldsymbol{0} \\ \hline \boldsymbol{0} & \boldsymbol{P}^{-1} \end{array}\right)\boldsymbol{S}. \tag{21}$$

This equation shows that $\frac{\partial \boldsymbol{x}}{\partial \boldsymbol{k}}$, which is located in the first M rows of the sensitivity matrices, is the same for $\boldsymbol{S}$ and $\boldsymbol{S}'$. The sensitivity of each flux is given by Eq. (8) (since we are focusing on qualitative changes, we can assume $\frac{\partial r_j}{\partial k_n} = \pm\delta_{n,j}$), which is also the same between the two bases. ■

Lemma 1 guarantees that the sensitivities of chemical concentrations fluxes with respect to reaction rate parameters are not affected by the choice of a basis for $\ker \boldsymbol{\nu}$, which allows us to choose any basis we prefer. The following lemma provides one way to choose a basis for $\ker \boldsymbol{\nu}$.

Lemma 2. Let $\mathfrak{r}_\Gamma$ be a subset of reactions in a CRN. We let $V_{\mathfrak{r}_\Gamma} := \{\boldsymbol{x} \in \ker \boldsymbol{\nu} \mid \mathrm{supp}\,\boldsymbol{x} \subset \mathfrak{r}_\Gamma\}$. We also define $N(\mathfrak{r}_\Gamma) := \dim V_{\mathfrak{r}_\Gamma}$ as previously defined. If $\dim \ker \boldsymbol{\nu} \geqslant 1$, there exists a basis $\{\boldsymbol{f}_i\}_{i=1,\dots,K}$ for $\ker \boldsymbol{\nu}$ such that

(i) $\boldsymbol{f}_1, \dots, \boldsymbol{f}_{N(\mathfrak{r}_\Gamma)} \subset V_{\mathfrak{r}_\Gamma}$,

(ii) $\mathfrak{r}^c_\Gamma$-projected $\boldsymbol{f}_{N(\mathfrak{r}_\Gamma)+1}, \dots, \boldsymbol{f}_K$ are linearly independent.

By $\mathfrak{r}^c_\Gamma$-projected $\boldsymbol{f}_i$, we mean $\boldsymbol{P}^{\mathfrak{r}^c_\Gamma}\boldsymbol{f}_i$, where $\boldsymbol{P}^{\mathfrak{r}^c_\Gamma} \in \mathbb{R}^{N\times N}$ is a projection matrix satisfying

$$\boldsymbol{P}^{\mathfrak{r}^c_\Gamma}_{j,j'} = \delta_{j,j'} \text{ if } j, j' \in \mathfrak{r}^c_\Gamma. \text{ Otherwise } \boldsymbol{P}^{\mathfrak{r}^c_\Gamma}_{j,j'} = 0. \tag{22}$$

Proof of Lemma 2. If $N(\mathfrak{r}_\Gamma) = K$, the statement is trivial. We will focus on the case of $N(\mathfrak{r}_\Gamma) < K$. If $N(\mathfrak{r}_\Gamma) \geqslant 1$, we first choose a basis for $V_{\mathfrak{r}_\Gamma}$ as $\{\boldsymbol{f}_1, \dots, \boldsymbol{f}_{N(\mathfrak{r}_\Gamma)}\}$, which satisfies condition (i). Then, we add some vectors to the basis vectors such that $\{\boldsymbol{f}_1, \dots, \boldsymbol{f}_{N(\mathfrak{r}_\Gamma)}, \boldsymbol{f}_{N(\mathfrak{r}_\Gamma)+1}, \dots, \boldsymbol{f}_K\}$ forms a basis for $\ker \boldsymbol{\nu}$. The set $\{\boldsymbol{f}_{N(\mathfrak{r}_\Gamma)+1}, \dots, \boldsymbol{f}_K\}$ spans the complementary subspace of $V_{\mathfrak{r}_\Gamma}$, denoted by $V^c_{\mathfrak{r}_\Gamma}$. [If $N(\mathfrak{r}_\Gamma) = 0$, we can choose an arbitrary basis for $\ker \boldsymbol{\nu}$ as $\{\boldsymbol{f}_i\}_{i=1,\dots,K}$. In this case, $V^c_{\mathfrak{r}_\Gamma} = \{\boldsymbol{0}\}$.]

Let $\bar{\boldsymbol{f}}_i$ be the $\mathfrak{r}^c_\Gamma$-projected $\boldsymbol{f}_i$. We will prove that $\bar{\boldsymbol{f}}_{N(\mathfrak{r}_\Gamma)+1}, \dots, \bar{\boldsymbol{f}}_K$ are linearly independent. Suppose on the contrary that $\bar{\boldsymbol{f}}_{N(\mathfrak{r}_\Gamma)+1}, \dots, \bar{\boldsymbol{f}}_K$ are linearly dependent. Then, there exists $\{\alpha_i\}_{i=N(\mathfrak{r}_\Gamma)+1}^K$ (at least one of $\alpha_{N(\mathfrak{r}_\Gamma)+1}, \dots, \alpha_K$ is nonzero) such that $\alpha_{N(\mathfrak{r}_\Gamma)+1}\bar{\boldsymbol{f}}_{N(\mathfrak{r}_\Gamma)+1} + \cdots + \alpha_K\bar{\boldsymbol{f}}_K = \boldsymbol{0}$. We let $\boldsymbol{g} := \alpha_{N(\mathfrak{r}_\Gamma)+1}\boldsymbol{f}_{N(\mathfrak{r}_\Gamma)+1} + \cdots + \alpha_K\boldsymbol{f}_K$. Because the $\mathfrak{r}^c_\Gamma$-projected $\boldsymbol{g}$ is $\boldsymbol{0}$, we have $\boldsymbol{g} \in V(\mathfrak{r}_\Gamma)$. At the same time, $\boldsymbol{g} \in V(\mathfrak{r}_\Gamma)^c$ because $\boldsymbol{g}$ is written as a linear combination of $\boldsymbol{f}_{N(\mathfrak{r}_\Gamma)+1}, \dots, \boldsymbol{f}_K \in V(\mathfrak{r}_\Gamma)^c$. Therefore, $\boldsymbol{g} \in V(\mathfrak{r}_\Gamma) \cap V(\mathfrak{r}_\Gamma)^c = \{\boldsymbol{0}\}$, i.e., $\boldsymbol{g} = \boldsymbol{0}$. This implies that $\alpha_{N(\mathfrak{r}_\Gamma)+1}\boldsymbol{f}_{N(\mathfrak{r}_\Gamma)+1} + \cdots + \alpha_K\boldsymbol{f}_K = \boldsymbol{0}$, which contradicts the fact that $\boldsymbol{f}_{N(\mathfrak{r}_\Gamma)+1}, \dots, \boldsymbol{f}_K$ are linearly independent. This completes the proof of Lemma 2. ■

Proof of Theorem 3. Suppose a subnetwork $\Psi = (\mathfrak{m}_\Psi, \mathfrak{r}_\Psi)$ is a regulatory module. Since Ψ is an output-complete subnetwork, it suffices to show that $\lambda(\Psi) = 0$.

We choose $\{\boldsymbol{f}_i\}_{i=1,\dots,K}$ for $\ker \boldsymbol{\nu}$ as shown in Lemma 2. As shown below, by collecting the indices associated with $\Psi = (\mathfrak{m}_\Psi, \mathfrak{r}_\Psi)$ into the upper-left corner, $\boldsymbol{A}$ can be represented as a block matrix with the lower left corner being a zero matrix

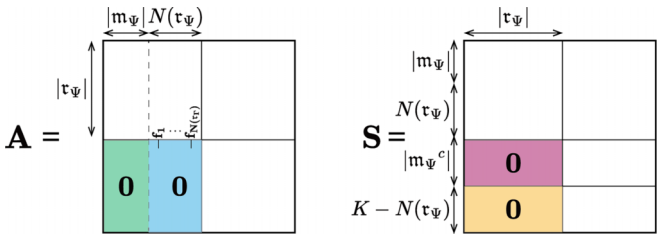

FIG. 2. Schematic depiction of $\boldsymbol{A}$ and $\boldsymbol{S}$ when $\Psi = (\mathfrak{m}_\Psi, \mathfrak{r}_\Psi)$ is a regulatory module. (Left) By collecting the indices associated with Ψ into the upper-left corner, $\boldsymbol{A}$ can be a block matrix in which the lower right is the zero matrix. (Right) The sensitivity matrix $\boldsymbol{S}$ is also proved to be a block matrix in which the lower right is the zero matrix. See proof of Theorem 3.

[Fig. 2 (left)]. The column indices in the upper-left block consist of the chemicals in $\mathfrak{m}_\Psi$ followed by $-\boldsymbol{f}_1, \ldots, -\boldsymbol{f}_{N(\mathfrak{r}_\Psi)}$, which are the basis vectors of $V_{\mathfrak{r}_\Psi} := \{\boldsymbol{x} \in \ker \boldsymbol{v} \mid \operatorname{supp} \boldsymbol{x} \subset \mathfrak{r}_\Gamma\}$. The row indices consist of the reactions in $\mathfrak{r}_\Psi$. All entries in the green region in Fig. 2 (left) are 0, because Ψ is output-complete. All entries in the blue region in Fig. 2 (left) are 0, because $\operatorname{supp} \boldsymbol{f}_i \subset \mathfrak{r}_\Psi$ $(i = 1, \ldots, N(\mathfrak{r}_\Psi))$. Since we are assuming $\det \mathbf{A} \neq 0$, the block associated with $\Psi = (\mathfrak{m}_\Psi, \mathfrak{r}_\Psi)$ in Fig. 2 (left) is vertically long or square; i.e., $\lambda(\Psi) = -|\mathfrak{m}_\Psi| + |\mathfrak{r}_\Psi| - N(\mathfrak{r}_\Psi) \geqslant 0$.

It remains to prove that $\lambda(\Psi) \leqslant 0$. $\boldsymbol{S} = -\boldsymbol{A}^{-1}$ is also in the block form in which the lower-left part is the zero matrix, as we will prove below [Fig. 2 (right)]. First, all $\frac{\partial x_m}{\partial k_n}$ with $m \in \mathfrak{m}_\Psi^c$ and $n \in \mathfrak{r}_\Psi$, which appear in the red region in Fig. 2 (right), vanish due to the assumption that the steady-state chemical concentrations in $\mathfrak{m}_\Psi^c$ do not change under perturbations of reaction rate parameters in $\mathfrak{r}_\Psi$. We next show that all $\frac{\partial \mu_l}{\partial k_n}$, with $\boldsymbol{f}_l \notin V_{\mathfrak{r}_\Psi}$ and $n \in \mathfrak{r}_\Psi$, which appear in the orange region in Fig. 2 (right), do not have nonzero entries. The change rate in the steady-state reaction flux vector in response to the perturbation to k_n is given by

$$\frac{\partial \boldsymbol{r}}{\partial k_n} = \frac{\partial \mu_1}{\partial k_n}\boldsymbol{f}_1 + \cdots + \frac{\partial \mu_K}{\partial k_n}\boldsymbol{f}_K, \quad n = 1, \ldots, N. \tag{23}$$

Recall that the reaction fluxes outside of a regulatory module Ψ remain unchanged under either perturbations of reaction rate parameters in Ψ (Remark 2). This means that

$$\mathbf{0} = \frac{\partial \mu_1}{\partial k_n}\bar{\boldsymbol{f}}_1 + \cdots + \frac{\partial \mu_K}{\partial k_n}\bar{\boldsymbol{f}}_K, \quad \forall n \in \mathfrak{r}_\Psi, \tag{24}$$

where $\bar{\boldsymbol{f}}_1, \ldots, \bar{\boldsymbol{f}}_K$ are $\mathfrak{r}_\Psi^c$-projected $\boldsymbol{f}_1, \ldots, \boldsymbol{f}_K$. From Lemma 2 (i), $\boldsymbol{f}_1, \ldots, \boldsymbol{f}_{N(\mathfrak{r}_\Psi)}$ have nonzero values only in $\mathfrak{r}_\Psi$, so $\bar{\boldsymbol{f}}_1, \ldots, \bar{\boldsymbol{f}}_{N(\mathfrak{r}_\Psi)}$ are all $\mathbf{0}$. Thus we obtain

$$\mathbf{0} = \frac{\partial \mu_{N(\mathfrak{r}_\Psi)+1}}{\partial k_n}\bar{\boldsymbol{f}}_{N(\mathfrak{r}_\Psi)+1} + \cdots + \frac{\partial \mu_K}{\partial k_n}\bar{\boldsymbol{f}}_K, \quad \forall n \in \mathfrak{r}_\Psi. \tag{25}$$

By Lemma 2 (ii), $\bar{\boldsymbol{f}}_{N(\mathfrak{r}_\Psi)+1}, \ldots, \bar{\boldsymbol{f}}_K$ are linearly independent, which implies that

$$\frac{\partial \mu_{N(\mathfrak{r}_\Psi)+1}}{\partial k_n} = \cdots = \frac{\partial \mu_K}{\partial k_n} = 0, \quad \forall n \in \mathfrak{r}_\Psi. \tag{26}$$

This completes the proof of the structure of $\boldsymbol{S}$.

Because $\boldsymbol{A}$ is invertible, $\boldsymbol{S}$ is also invertible. This implies that the upper-left block in Fig. 2 (right) is vertically long or square; i.e., $|\mathfrak{m}_\Psi| + N(\mathfrak{r}_\Gamma) \geqslant |\mathfrak{r}_\Psi|$, thus $\lambda(\Psi) \leqslant 0$, which completes the proof. ■

ALGORITHM 1. Finding all buffering structures (for CRNs without conserved quantities).

Output: $\{Y_1, \ldots, Y_N\}$, where $Y_n = \{\mathfrak{m}_{Y_n}, \mathfrak{r}_{Y_n}\}$ ($\mathfrak{m}_{Y_n}$ is the set of chemicals and $\mathfrak{r}_{Y_n}$ is the set of reactions).
1: $\boldsymbol{S} \leftarrow -\boldsymbol{A}^{-1}$
2: **for** $n = 1, \ldots, N$ **do**
3: $\quad \mathfrak{m}_{Y_n} \leftarrow \{\}$, $\mathfrak{r}_{Y_n} \leftarrow \{n\}$
4: $\quad \mathfrak{m}_{Y_n} \leftarrow M(\mathfrak{r}_{Y_n})$
5: $\quad \mathfrak{r}_{Y_n} \leftarrow \mathfrak{r}_{Y_n} \cup R(\mathfrak{m}_{Y_n})$
6: $\quad Y_n \leftarrow \{\mathfrak{m}_{Y_n}, \mathfrak{r}_{Y_n}\}$
7: **end for**
8: **return** $\{Y_1, \ldots, Y_N\}$

IV. THE ALGORITHM TO FIND BUFFERING STRUCTURES

In this section, we present the algorithm to enumerate buffering structures. Similar to the previous section, we will consider CRNs that lack conserved quantities (see Appendix A for the general case). From Theorem 4, finding buffering structures is equivalent to finding regulatory modules. For each reaction n, we find the minimum buffering structure containing the reaction n through the following procedures (Algorithm 1).

We first calculate the zero distribution of $\boldsymbol{S} := -\boldsymbol{A}^{-1}$. Then, for each reaction n, we calculate $M(n)$, defined as the set of chemicals that are influenced by the reaction n, i.e., $M(n) := \{m \mid \frac{\partial x_m}{\partial k_n} \neq 0\}$. For a reaction set $\mathcal{N}$, we let $M(\mathcal{N}) := \bigcup_{n\in\mathcal{N}} M(n)$. For a chemical m, we let $R(m)$ be the set of reactions whose reaction rates are dependent on m, i.e., $R(m) := \{n \mid \frac{\partial r_n}{\partial x_m} \neq 0\}$. Intuitively, $R(m)$ is the set of edges (reaction arrows) that leave the node (chemical) m in the graph. For a chemical set $\mathfrak{m}$, we let $R(\mathfrak{m}) := \bigcup_{m\in\mathfrak{m}} R(m)$.

To obtain the minimum buffering structure that contains the reaction n, we first construct a subnetwork that contains only reaction n. Then, we add to the subnetwork $M(n)$, whose steady-state concentrations are affected by the perturbation to the reaction n. The subnetwork can be made output-complete by adding $R(M(n)) \setminus \{n\}$. From the transitivity property (Remark 3, below), the perturbations to the newly added reactions $R(M(n)) \setminus \{n\}$ do not affect the steady-state concentration of any chemical outside the subnetwork. Hence, the resulting subnetwork Y_n is a regulatory module and thus a buffering structure from Theorem 3. It is clear that Y_n is the minimum buffering structure containing the reaction n. We iterate the procedure for $n = 1, \ldots, N$ and remove duplicates, obtaining $Y_{p_1}, \ldots, Y_{p_s}$ $(1 \leqslant p_1 < \cdots < p_s \leqslant N)$.

Remark 3. If the system does not have the conserved quantities, the transitivity property for influences was proved [34]. If r_1 influences m_1, the reaction rate of r_2 is dependent on m_1, and the r_2 influences m_2, then r_1 influences m_2. In symbols,

$$r_1 \rightsquigarrow m_1 \mapsto r_2 \rightsquigarrow m_2 \Rightarrow r_1 \rightsquigarrow m_2. \tag{27}$$

Here, $r \rightsquigarrow m$ means that the reaction r influences the chemical m and $m \mapsto r$ means that the reaction rate of r is dependent on the concentration of m.

From Algorithm I, we obtain the following theorem.

Theorem 5. If the system does not have the conserved quantity, the reaction n influences all chemicals in Y_n.

There exist buffering structures other than the aforementioned $Y_{p_1}, \ldots, Y_{p_s}$. However, the set $\{Y_{p_1}, \ldots, Y_{p_s}\}$ covers all buffering structures in a CRN in the sense that $\{Y_{p_1}, \ldots, Y_{p_s}\}$ is the "minimum set of buffering structures" defined as follows.

Definition 4. (Minimum set of buffering structures). A set of buffering structures $\{\Gamma_1, \ldots, \Gamma_s\}$ is the "minimum set of buffering structures" of a regular CRN if

(1) For any buffering structure Γ of the CRN, there exists $1 \leqslant n_1 < \cdots < n_m \leqslant s$ such that $\Gamma = \Gamma_{n_1} \cup \cdots \cup \Gamma_{n_m}$.

(2) Each Γ_i cannot be expressed as a union of smaller buffering structures, i.e., for any i ($1 \leqslant i \leqslant s$), there cannot exist nonempty buffering structures Γ' and Γ'' ($\Gamma' \subsetneq \Gamma_i$ and $\Gamma'' \subsetneq \Gamma_i$) such that $\Gamma_i = \Gamma' \cup \Gamma''$.

Theorem 6. $\{Y_{p_1}, \ldots, Y_{p_s}\}$ is the minimum set of buffering structures.

Proof of Theorem 6. We first prove that $\{Y_{p_1}, \ldots, Y_{p_s}\}$ satisfies condition (1) of Definition 4. Suppose on the contrary that there exists a buffering structure $\Gamma = (\mathfrak{m}_\Gamma, \mathfrak{r}_\Gamma)$ that does not satisfy the condition. If Γ contains no reactions, $|\mathfrak{r}_\Gamma| = |\mathfrak{m}_\Gamma| + N(\mathfrak{r}_\Gamma) = 0$, hence $|\mathfrak{m}_\Gamma| = 0$ and Γ is empty. Therefore we only consider the case where Γ contains at least one reaction. Let $\{n_1, \ldots, n_q\}$ be the set of reactions in $\mathfrak{r}_\Gamma$. For $i = 1, \ldots, q$, Γ includes the minimum buffering structure containing the reaction n_i, hence we have $\Gamma \supset \sigma$, where $\sigma = Y_{n_1} \cup \cdots \cup Y_{n_q}$. Because $\sigma = (\mathfrak{m}_\sigma, \mathfrak{r}_\sigma)$ is a buffering structure, $|\mathfrak{m}_\sigma| - |\mathfrak{r}_\sigma| + N(\mathfrak{r}_\sigma) = 0$. Since the reaction set in σ is the same as that in Γ, $|\mathfrak{r}_\sigma| = |\mathfrak{r}_\Gamma|$ and $N(\mathfrak{r}_\sigma) = N(\mathfrak{r}_\Gamma)$. Because $|\mathfrak{m}_\Gamma| - |\mathfrak{r}_\Gamma| + N(\mathfrak{r}_\Gamma) = 0$, we have $|\mathfrak{m}_\sigma| = |\mathfrak{m}_\Gamma|$. Since $\mathfrak{m}_\sigma \subset \mathfrak{m}_\Gamma$, we have $\mathfrak{m}_\sigma = \mathfrak{m}_\Gamma$ and thus $\sigma = \Gamma$, which means that $\Gamma = Y_{n_1} \cup \cdots \cup Y_{n_q}$, contradicting the assumption.

We finally prove that $\{Y_{p_1}, \ldots, Y_{p_s}\}$ satisfies condition (2) of Definition 4. Suppose for some $i \in \mathbb{N}$ ($1 \leqslant i \leqslant s$), there exists two nonempty buffering structures Γ' and Γ'' ($\Gamma' \subsetneq Y_{p_i}$ and $\Gamma'' \subsetneq Y_{p_i}$) such that $Y_{p_i} = \Gamma' \cup \Gamma''$. Since $p_i \subset Y_{p_i}$, it holds that $p_i \in \Gamma'$ or $p_i \in \Gamma''$. We can assume $p_i \in \Gamma'$ without loss of generality. Then, we have $Y_{p_i} \subset \Gamma'$. At the same time, since Γ' and Γ'' are nonempty, we have $Y_{p_i} \supsetneq \Gamma'$, a contradiction. ∎

Computational complexity. A naive algorithm to check whether a given subnetwork in a CRN conforms to the definition of BS (Definition 2) for all subnetworks has an exponential time complexity of $O(2^{M+N})$. In contrast, the most time-consuming step of our proposed approach is the calculation of $\boldsymbol{S} = -\boldsymbol{A}^{-1}$. Although symbolic calculation of the inverse matrix is infeasible for a large-sized matrix, the distribution of zero entries in the inverse of a sparse matrix can be estimated numerically [34]. We assign random values to $r_{j,m}$ ($\neq 0$) appearing in $\boldsymbol{A}$ and numerically calculate $\boldsymbol{A}^{-1}$. We repeat this process multiple times to determine the distribution of zero entries in $\boldsymbol{S}$. The time complexity of this procedure is $O(N^3)$, which is much lower than the brute-force method.

We illustrate our algorithm with some example networks.

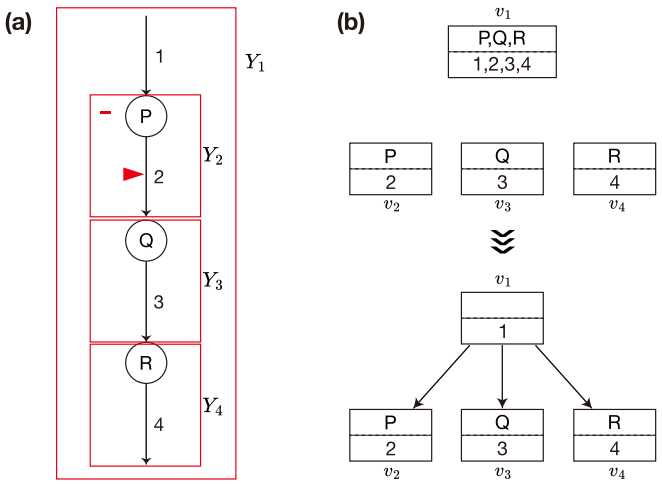

FIG. 3. Analysis for a hypothetical network (Example 2). (a) Graphical representation of a CRN with three chemicals (P, Q, R) and four reactions (1, 2, 3, 4). Solid lines indicate chemical reactions. Each subnetwork enclosed by a red box (Y_i) represents a minimum buffering structure containing the reaction i. (b) The hierarchy graph. Initially, we construct a graph where each Y_i is assigned to a node v_i. Modulating the enzyme activity of reactions within a box can lead to nonzero responses in the chemicals within that box and those in the lower boxes, while leaving the other chemicals unaffected. The set of nodes in the hierarchy graph provides the disjoint decomposition of the CRN.

Example 2. We consider a straight pathway, shown in Fig. 3(a), which is the same as the pathway in Fig. 1(a). As shown in Eq. (16), the sensitivity is given by

$$\mathbf{S} = -\mathbf{A}^{-1} = \begin{pmatrix} * & * & 0 & 0 \\ * & 0 & * & 0 \\ * & 0 & 0 & * \\ * & 0 & 0 & 0 \end{pmatrix}, \tag{28}$$

where $*$ represents a nonzero response. We will exhaustively search for buffering structures in the CRN. Using the sensitivity matrix, we obtain M(r): $M(1) = \{\text{P, Q, R}\}$, $M(2) = \{\text{P}\}$, $M(3) = \{\text{Q}\}$, $M(4) = \{\text{R}\}$.

We also obtain $R(m)$, which is the set of edges (reaction arrows) that leave the node (chemical) m in the graph: $R(\text{P}) = \{2\}$, $R(\text{Q}) = \{3\}$, $R(\text{R}) = \{4\}$.

Since this system does not have conserved quantities, the minimum set of buffering structures is given by Algorithm I [Fig. 3(a)]: $Y_1 = \{\{\text{P, Q, R}\}, \{1, 2, 3, 4\}\}$, $Y_2 = \{\{\text{P}\}, \{2\}\}$, $Y_3 = \{\{\text{Q}\}, \{3\}\}$, $Y_4 = \{\{\text{R}\}, \{4\}\}$.

Example 3. We consider a hypothetical pathway, shown in Fig. 4(a). The stoichiometric matrix is given by

$$\boldsymbol{\nu} = \begin{pmatrix} 1 & -1 & 0 & 1 & 0 & 0 & 0 & 0 \\ 0 & 1 & -1 & 0 & 1 & 0 & 0 & 0 \\ 0 & 0 & 1 & 0 & 0 & -1 & 0 & 0 \\ 0 & 0 & 0 & -1 & 0 & 0 & -1 & 0 \\ 0 & 0 & 0 & 0 & -1 & -1 & 1 & 0 \\ 0 & 0 & 0 & 0 & 0 & 1 & 0 & -1 \end{pmatrix}. \tag{29}$$

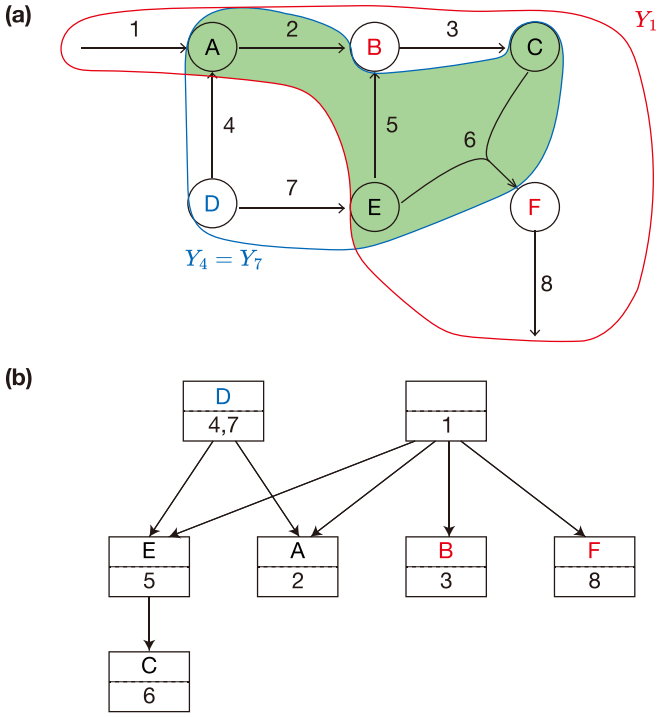

FIG. 4. Analysis for a hypothetical network (Example 3). (a) Graphical representation of a CRN with 6 chemicals (A, . . . , F) and 8 reactions (1, . . . , 8). Solid lines indicate chemical reactions. Y_1 is shown in red, and $Y_4 = Y_7$ is shown in blue. The intersection of these two is colored in green, which is also a buffering structure. (b) The hierarchy graph. Modulating the enzyme activity of reactions within a box leads to nonzero responses in the chemicals within that box and those in the lower boxes, leaving the other chemicals unaffected.

Since $\boldsymbol{v}$ has kernel vectors $\boldsymbol{c}_1 = (0, -1, 0, -1, 1, 0, 1, 0)^\top, \boldsymbol{c}_2 = (2, 2, 1, 0, -1, 1, 0, 1)^\top$ (note that $M = 6$, $K = 2$, and $N = 8$, and hence $M + K = N$, implying that the CRN does not have the conserved quantities), the matrix $\mathbf{A}$ is

$$\mathbf{A} = \begin{pmatrix} 0 & 0 & 0 & 0 & 0 & 0 & 0 & -2 \\ r_{2,\mathrm{A}} & 0 & 0 & 0 & 0 & 0 & 1 & -2 \\ 0 & r_{3,\mathrm{B}} & 0 & 0 & 0 & 0 & 0 & -1 \\ 0 & 0 & 0 & r_{4,\mathrm{D}} & 0 & 0 & 1 & 0 \\ 0 & 0 & 0 & 0 & r_{5,\mathrm{E}} & 0 & -1 & 1 \\ 0 & 0 & r_{6,\mathrm{C}} & 0 & r_{6,\mathrm{E}} & 0 & 0 & -1 \\ 0 & 0 & 0 & r_{7,\mathrm{D}} & 0 & 0 & -1 & 0 \\ 0 & 0 & 0 & 0 & 0 & r_{8,\mathrm{F}} & 0 & -1 \end{pmatrix}, \tag{30}$$

and the sensitivity is determined as

$$\mathbf{S} = -\mathbf{A}^{-1} = \begin{pmatrix} * & * & 0 & * & 0 & 0 & * & 0 \\ * & 0 & * & 0 & 0 & 0 & 0 & 0 \\ * & 0 & 0 & * & * & * & * & 0 \\ 0 & 0 & 0 & * & 0 & 0 & * & 0 \\ * & 0 & 0 & * & * & 0 & * & 0 \\ * & 0 & 0 & 0 & 0 & 0 & 0 & * \\ 0 & 0 & 0 & * & 0 & 0 & * & 0 \\ * & 0 & 0 & 0 & 0 & 0 & 0 & 0 \end{pmatrix}, \tag{31}$$

where $*$ represents a nonzero response.

Using the sensitivity matrix, we obtain $M(r)$: $M(1) = \{\mathrm{A}, \mathrm{B}, \mathrm{C}, \mathrm{E}, \mathrm{F}\}$, $M(2) = \{\mathrm{A}\}$, $M(3) = \{\mathrm{B}\}$, $M(4) = \{\mathrm{A}, \mathrm{C}, \mathrm{D}, \mathrm{E}\}$, $M(5) = \{\mathrm{C}, \mathrm{E}\}$, $M(6) = \{\mathrm{C}\}$, $M(7) = \{\mathrm{A}, \mathrm{C}, \mathrm{D}, \mathrm{E}\}$, $M(8) = \{\mathrm{F}\}$.

We also obtain $R(m)$, which is the set of edges (reaction arrows) that leave the node (chemical) m in the graph: $R(\mathrm{A}) = \{2\}$, $R(\mathrm{B}) = \{3\}$, $R(\mathrm{C}) = \{6\}$, $R(\mathrm{D}) = \{4, 7\}$, $R(\mathrm{E}) = \{5, 6\}$, $R(\mathrm{F}) = \{8\}$.

Since this system does not have conserved quantities, the minimum set of buffering structures is given by Algorithm 1 [Fig. 4(a)]: $Y_1 = \{\{\mathrm{A}, \mathrm{B}, \mathrm{C}, \mathrm{E}, \mathrm{F}\}, \{1, 2, 3, 5, 6, 8\}\}$, $Y_2 = \{\{\mathrm{A}\}, \{2\}\}$, $Y_3 = \{\{\mathrm{B}\}, \{3\}\}$, $Y_4 = Y_7 = \{\{\mathrm{A}, \mathrm{C}, \mathrm{D}, \mathrm{E}\}, \{2, 4, 5, 6, 7\}\}$, $Y_5 = \{\{\mathrm{C}, \mathrm{E}\}, \{5, 6\}\}$, $Y_6 = \{\{\mathrm{C}\}, \{6\}\}$, $Y_8 = \{\{\mathrm{F}\}, \{8\}\}$.

Parameters that influence D and those that affect B (or F) are disjoint, hence D and B (or F) are independently regulated. This is explained by the presence of two buffering structures. B and F are part of Y_1 [Fig. 4(a) red], hence the reactions in Y_1 influences only chemicals within Y_1, including B and F. D is part of $Y_4 = Y_7$ [Fig. 4(a) blue], hence the reactions in $Y_4 = Y_7$ influences only chemicals within $Y_4 = Y_7$, including D. These two buffering structures have an intersection [Fig. 4(a) green], including the reactions 2, 5, and 6. From Proposition 1, the intersection is also a buffering structure, indicating that the reactions in the intersection do not influence B, D, or F. Thus, the reactions influencing D and those affecting B (or F) are disjoint. This is an example where multiple chemicals in a single connected CRN are independently regulated through buffering structures.

V. HIERARCHY GRAPH

We previously found that the nonzero response patterns under perturbations of different parameters can exhibit inclusion relations among them, i.e., exhibit hierarchical structures [12,14]. This hierarchy encompasses every possible perturbation-response pattern. In addition, it was previously shown that buffering structures exhibit a hierarchy [12]. In what follows, we show that the hierarchy of perturbation-response patterns corresponds to that of buffering structures. We also present a method to graphically illustrate the hierarchy.

We are able to construct a hierarchy graph of nonzero response patterns in the following way. We obtain $Y_{p_1}, \ldots, Y_{p_s}$ in the same way as Sec. IV. Each $Y_{p_i} = (\mathfrak{m}_{Y_{p_i}}, \mathfrak{r}_{Y_{p_i}})$ represents a perturbation-response relationship, i.e., perturbations to parameters in $\mathfrak{r}_{Y_{p_i}}$ are confined to $\mathfrak{m}_{Y_{p_i}}$. In the following way, we construct the graph $G = (\{v_i\}_{i=1}^s, E)$ representing the inclusion relationship of $Y_{p_1}, \ldots, Y_{p_s}$.

(1) We initially prepare a set of nodes $\{v_i\}_{i=1}^s$. Y_{p_i} is assigned to v_i. The edge set E is empty at this time.

(2) For any pair of i and j ($1 \leqslant i, j \leqslant s$), we add an edge $v_j \to v_i$ if $Y_{p_i} \subsetneqq Y_{p_j}$. (3) For any pair of i and j ($1 \leqslant i, j \leqslant s$), we remove an edge $v_j \to v_i$ if there exists the path from v_j to v_i of length greater than or equal to 2. The graph G is a directed acyclic graph (if $v_1 \to \ldots \to v_q$ forms a cycle, $Y_{p_1} = \cdots = Y_{p_q}$, which contradicts the fact that duplicates in $\{Y_{p_1}, \ldots, Y_{p_s}\}$ are removed).

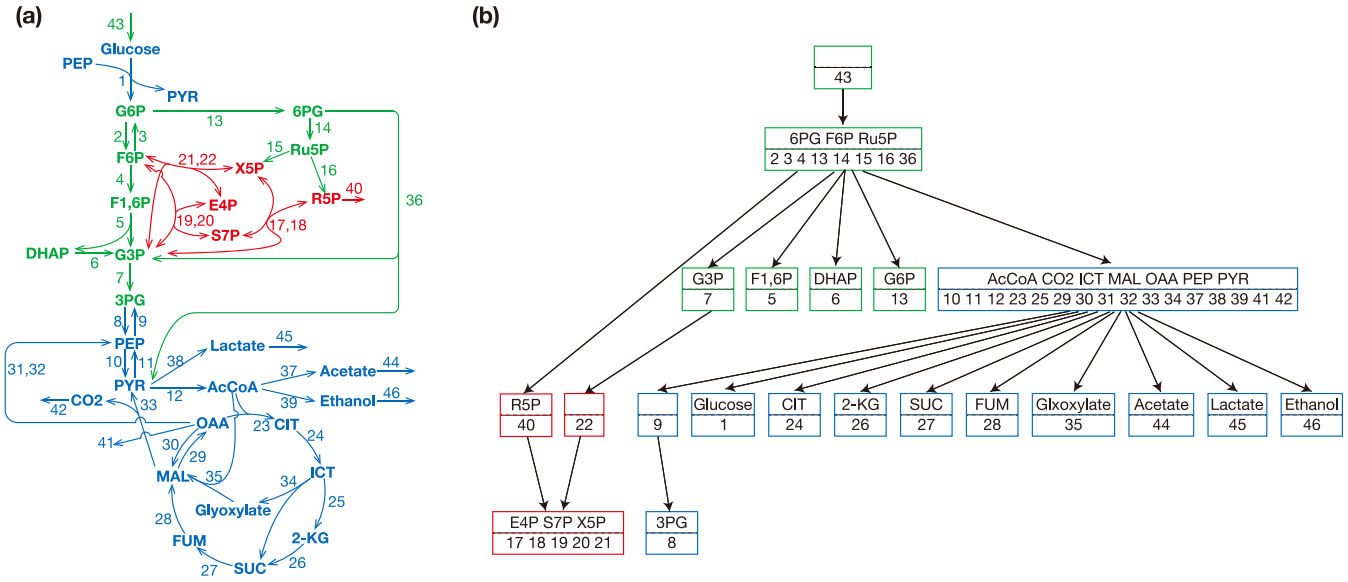

FIG. 5. Analysis for a metabolic network of *E. coli*, including glycolysis, the pentose phosphate pathway (PPP), and the tricarboxylic acid (TCA) cycle (Example 4). (a) Graphical representation of a CRN. (b) The hierarchy graph of the CRN in (a). The red part highlights a portion of the PPP, which is a buffering structure. The blue part encompasses the TCA cycle, which is also a buffering structure. The green part corresponds to the glycolysis pathway, positioned at the apex of the hierarchy.

(4) We let $Z_i := Y_{p_i} - \bigcup_{j\in D_i} Y_{p_j}$, where D_i is the union of nodes that are downstream of v_i. We change the assignment of v_i from Y_{p_i} to Z_i.

The resulting hierarchy graph G represents the inclusion relationship between buffering structures. The union of each node v_i with its downstream nodes D_i forms a distinct buffering structure. Furthermore, Theorem 6 demonstrates that all buffering structures are represented by a union of a node and its downstream nodes. This implies that any node cannot be further decomposed into smaller nodes.

The hierarchy graph G also summarizes the nonzero response patterns. According to Theorem 5, perturbations to any parameter within a node influence not only chemicals within that node but also those in its downstream nodes.

Remark 4. The influential relationships between Z_i and Z_j are all or none. There are only two possibilities: (i) The perturbation to any parameter in Z_i affects all chemicals in Z_j, or (ii) no parameter in Z_i has any effect on the chemicals in Z_j. This allows us to define the relation $\twoheadrightarrow$, with $Z_i \twoheadrightarrow Z_j$ meaning that the perturbation to parameters in Z_i affects all chemicals in Z_j. Then, $(\{Z_i\}_{i=1}^s, \twoheadrightarrow)$ is a partially ordered set, and G illustrates its hierarchical order.

The set of nodes in G is a disjoint set, as shown in the following theorem.

Theorem 7. In the hierarchy graph G, every chemical and reaction appears exactly once.

Proof of Theorem 7. Because Y_i contains reaction i, every reaction appears at least once. From the regularity of the matrix $\boldsymbol{A}$, $\boldsymbol{S}$ is invertible, thus, every chemical is influenced by at least one reaction. Hence, all chemicals appear in G more than once.

Suppose G has two distinct nodes v_i and v_j such that $Z_i \cap Z_j \neq \emptyset$. We pick $e \in Z_i \cap Z_j$ (e is either a chemical or a reaction). Since $Z_i \subset Y_{p_i}$ and $Z_j \subset Y_{p_j}$, we have $e \in Y_{p_i} \cap Y_{p_j}$. Because both Y_{p_i} and Y_{p_j} are buffering structures, their intersection $Y_{p_i} \cap Y_{p_j}$ is also a buffering structure by Proposition 1. Thus, according to Theorem 6, there exist buffering structures $Y_{q_1}, \ldots, Y_{q_l}$ such that $Y_{p_i} \cap Y_{p_j} = Y_{q_1} \cup \cdots \cup Y_{q_l}$. There exists k ($1 \leqslant k \leqslant l$) such that $e \in Y_{q_k}$. Since $Y_{q_k} \subsetneq Y_{p_i}$, the node v_k is located downstream of v_i, implying that $Z_i \cap Y_{q_k} = \emptyset$. However, this contradicts the assumption that $e \in Z_i$ and $e \in Y_{q_k}$. This completes the proof of Theorem 7. ■

The proof of Theorem 7 is based on the fact that the intersection of two distinct buffering structures is also a buffering structure (Proposition 1). Theorem 7 indicates that if two distinct parameters both affect a common set of chemicals, then there exists a buffering structure that encompasses the common set of chemicals, with no additional chemicals included. Theorem 7 also suggests that the hierarchy graph G provides the disjoint decomposition $\bigcup_{i=1}^s Z_i$ for any CRN. The number of pieces in the decomposition is less than or equal to the number of parameters, because each node includes at least one parameter.

We illustrate our results in the toy networks [Example 2 in Fig. 3(b) and Example 3 in Fig. 4(b)] and a biological network [Example 4 in Fig. 5(b)].

Example 4. We present a metabolic network of *Escherichia coli*, including multiple biologically identified subcircuits: the glycolysis pathway, the pentose phosphate pathway (PPP), and the tricarboxylic acid (TCA) cycle [Fig. 5(a), see Appendix B for the detail] [4,12,14]. The hierarchy graph of this CRN is shown in Fig. 5(b). Some of the nodes in the hierarchy graph, derived from the network topology, coincide remarkably with biologically identified subcircuits. A subset of PPP (red), which includes the nucleotide precursor Ribose-5-phosphate (R5P), forms a buffering structure, and the TCA cycle constitutes another buffering structure (blue). The glycolysis pathway (green) is positioned at the top of the hierarchy. This hierarchy suggests that while the activation of the glycolysis pathway influences

all subcircuits, the activation of the nucleotide synthesis pathway in PPP or the TCA cycle does not impact the other subcircuits.

One important implication of a hierarchy graph is that clear upstream and downstream relationships can always be identified through the hierarchical graph, regardless of the CRN's configuration. Even if a CRN has feedback loops and lacks a tree structure, its hierarchical graph never includes feedback loops. For instance, the central metabolic network (Example 4) has feedback mechanisms. Here, glycolysis products serve as precursors for the TCA cycle. At the same time, a TCA-derived chemical (PEP) reenters the glycolysis pathway. Nevertheless, its hierarchical graph does not have feedback loops. The glycolysis pathway is positioned upstream of the TCA cycle, with no path from the TCA cycle to the glycolysis pathway, indicating that, in terms of perturbation-response relationships, the glycolysis pathway is completely upstream to the TCA cycle.

Another implication of a hierarchy graph is the transitivity of influence. If a perturbation of parameters in a node 1 influences the chemicals in a node 2, and a perturbation of parameters in the node 2 influences the chemicals in a node 3, then a perturbation of parameters in the node 1 will also affect the chemicals in the node 3. In the hierarchy graphs of biological networks, each node can correspond to a specific subcircuit (Example 4). Suppose we know that perturbing a subcircuit 1 influences a subcircuit 2, yet the effect on a subcircuit 3 remains uncertain. If we know that the subcircuit 2 influences the subcircuit 3, then we can infer that a perturbation to the subcircuit 1 affects the subcircuit 3 as well.

VI. DISCUSSION

We previously demonstrated that the response of a CRN to the modulations of parameters can be determined solely from the local structure of the network [12,13]. When a subnetwork within a CRN satisfies specific topological conditions, it is denoted as a "buffering structure". The influence of a parameter perturbation within a buffering structure is confined within it (the "law of localization"). A buffering structure represents a novel concept in CRNs: a "regulatory module" can naturally arise from the topology of a network.

In previous studies [12,13], an *ad hoc* method was employed where buffering structures are identified by searching for an output-complete subnetworks that shows confined responses, based on SSA. However, it remained unclear whether all subnetworks exhibiting these properties satisfy the topological conditions of buffering structures. Our present study proves that an output-complete subnetwork displaying a finite-response range is always a buffering structure. This shows that buffering structures can be computed without redundancy by searching for output-complete subnetworks that exhibit confined responses. A naive algorithm to check whether, for all subnetworks, a given subnetwork in a CRN conforms to the definition of a buffering structure, i.e., exhibits output-completeness and has an index of zero, has an exponential time complexity. In contrast, our proposed approach has polynomial time complexity.

The existence of a hierarchy among the nonzero responses to parameter perturbations has been hinted at in prior studies [12,14]. However, the connection between this hierarchy of nonzero responses and that of buffering structures remained elusive. Our research elucidates that the hierarchy among nonzero responses is equivalent to the hierarchy of buffering structures. Furthermore, we propose an algorithm to depict this hierarchy graphically through the computation of buffering structures.

This method can be applied to any CRN as long as the $\boldsymbol{A}$ matrix is invertible. Our approach equips researchers to explore buffering structures across various biological CRNs, including metabolic systems and signal transduction networks. This will clarify how different physiological functions emerging from a single CRN can be separately regulated.

In addition to sensitivities, the qualitative change (i.e., plasticity) of behaviors is another important aspect of biological systems. From a mathematical perspective, the discontinuous transition from one state to another in response to parameter perturbations can be understood within the framework of bifurcation theory of dynamical systems. Previously, two of the authors of this study introduced a method to study bifurcations of CRNs based solely on network topology, termed "structural bifurcation analysis" (SBA) [35,36]. SBA was developed upon an equivalence between the Jacobian matrix $\boldsymbol{J}$ of a reaction system and the augmented matrix $\boldsymbol{A}$, enabling bifurcation analysis based on network information. An important step in SBA involves decomposing a CRN according to the inclusion relationship among buffering structures. Our algorithm presented in this study for enumerating buffering structures and constructing their hierarchy will be useful for executing SBA.

The inverse theorem offers the potential utility for correcting the network information when combined with perturbation experiments. A vast amount of information about metabolic networks is available in databases [37–42], but the information of networks in these databases might be still incomplete: there might exist unidentified reactions or regulations. By perturbing metabolic enzymes and experimentally measuring the responses, it will be possible to identify the subnetwork that exhibits a confined response range. The index of such a subnetwork should be zero according to our inverse theorem. If the index calculated from the database network is not zero, modifications should be made to the network to ensure that the index is zero. By employing this strategy, it may be possible in the future to refine the metabolic networks in databases.

Our findings will pave the way to design a network that has certain buffering properties, ensuring consistent functionality despite various external and internal disturbances, which is crucial in synthetic biology [43–46]. The inverse theorem indicates that a subnetwork exhibiting a buffering property should display a zero index. Thus, we are able to design a subnetwork exhibiting a buffering property by targeting a zero index. If a subnetwork of a biological network has a positive index, it lacks the buffering properties, but network modifications to reduce the index to zero could endow it with such properties. The insights provided by Ref. [47], which reveals the patterns of index changes resulting from the addition of outflows to chemicals, may offer guidance on potential network modifications.

From a medical point of view, our algorithm for identifying buffering structures might be useful for elucidating the mechanisms underlying drug resistance. Drugs designed to

treat diseases, such as cancer, operate by inhibiting enzyme activity within CRNs. The extent of the molecular response induced by drugs could be defined by the buffering structure. It is plausible that, as cancer progresses, the structure of the CRN changes, leading to changes in buffering structures. If buffering structures narrow down, the effects of drug could get weaker, thereby inducing drug resistance. By comparing the buffering structures of normal tissues and those of cancerous CRNs, we may be able to identify the CRN changes that are key to drug resistance.

Hirono *et al.* proved the inverse theorem independently of us [22]. In our study, we not only proved the inverse theorem but also clarified the relationship between the hierarchy of nonzero responses and that of buffering structures.

One limitation of this study is that we have only discussed the case where the system is regular, i.e., the $\boldsymbol{A}$ matrix is invertible. When the system is not regular, we conjecture that structurally stable fixed points may not exist. If so, the $\boldsymbol{A}$ matrix in the actual biological CRNs should be invertible given that structurally stable fixed points are likely to exist. However, we observed that the $\boldsymbol{A}$ matrix calculated from the information in CRN databases is sometimes singular. One possibility is that network information within these databases may contain missing reactions or regulations. It is thus promising to develop a method to identify subnetworks that are predicted to be robust buffering structures even under possible network modifications.

In summary, we have developed an efficient method for exhaustively identifying buffering structures in any given CRN. This method is expected to lead to a better understanding of the basis for the independent regulation of different functions arising from a single connected CRN.

The Python implementation of ibuffpy is available at GitHub [48].

ACKNOWLEDGMENTS

We thank Yong-Jin Huang and Masato Ishikawa for their helpful discussions and comments. This research was supported by the CREST program (Grant no. JPMJCR1922) of the Japan Science and Technology Agency (JST), Grant-in-Aid for Scientific Research on Innovative Areas (Grants No. 19H03196, No. 19H05670), Joint Usage/Research Center Program of Institute for Life and Medical Sciences Kyoto University. Y.Y. was supported by JSPS KAKENHI (Grant No. 23K14156). T.O. was supported by JSPS KAKENHI (Grants No. 22K03453, No. 22K06347) and the RIKEN iTHEMS Program. A.H. was supported by JSPS KAKENHI (Grant No. 23KJ1324).

Y.Y. designed the study, provided mathematical proofs for the theorems, and wrote the manuscript. A.H. implemented the algorithm, and Y.Y also contribute to the implementation. T.O and A.M. contributed to the supervision of the study and the writing of the manuscript. Y.Y. wrote the manuscript with assistance from the other authors.

APPENDIX A: CRNs WITH CONSERVED QUANTITIES

1. Structural sensitivity analysis with conserved quantities

In the main text, we assumed that the system does not have the conserved quantities, i.e., $\dim\ker \boldsymbol{v}^\top = 0$, and thus $M + K = N$. In Ref. [13], SSA is generalized to CRNs with conserved quantities, which allows us to study any CRNs. We denote a basis of $\ker \boldsymbol{v}^\top$ (the cokernel basis) as $\{\boldsymbol{d}_a\}_{a=1}^{L}$, where $L \coloneqq \dim\ker \boldsymbol{v}^\top$. The quantity $\boldsymbol{d}_a^\top \boldsymbol{x} \equiv d_a$ remains constant throughout the dynamics (a conserved quantity), since $\frac{d}{dt}(\boldsymbol{d}_a^\top \boldsymbol{x}) = \boldsymbol{d}_a^\top \frac{d\boldsymbol{x}}{dt} = \boldsymbol{d}_a^\top \boldsymbol{v}\boldsymbol{r} = 0$. In the presence of conserved quantities, steady-state concentrations and fluxes are affected not only by reaction rate parameters but also by the initial values of conserved quantities. Therefore, in this case, there are two types of perturbations; the perturbation of the reaction rate parameter k_n and that of the conserved quantity d_a. To treat two types of perturbations in a unified way, we introduce generalized parameters J_i $(i = 1, \ldots, N + L)$ as

$$\{J_1, \ldots, J_N, J_{N+1}, \ldots, J_{N+L}\} \coloneqq \{k_1, \ldots, k_N, d_1, \ldots, d_L\}. \tag{A1}$$

We generalize the definition of $\boldsymbol{A}$ and $\tilde{\boldsymbol{S}}$ as follows:

$$\boldsymbol{A} \coloneqq \left(\begin{array}{ccc|ccc} r_{1,1} & \cdots & r_{1,M} & & & \\ \vdots & & \vdots & -\boldsymbol{c}_1 & \cdots & -\boldsymbol{c}_K \\ r_{N,1} & \cdots & r_{N,M} & & & \\ \hline & -\boldsymbol{d}_1^\top & & & & \\ & \vdots & & & \boldsymbol{0} & \\ & -\boldsymbol{d}_L^\top & & & & \end{array}\right), \tag{A2}$$

$$\tilde{\boldsymbol{S}} \coloneqq \left(\begin{array}{ccc|ccc} \frac{\partial x_1}{\partial J_1} & \cdots & \frac{\partial x_1}{\partial J_N} & \frac{\partial x_1}{\partial J_{N+1}} & \cdots & \frac{\partial x_1}{\partial J_{N+L}} \\ \vdots & & \vdots & \vdots & & \vdots \\ \frac{\partial x_M}{\partial J_1} & \cdots & \frac{\partial x_M}{\partial J_N} & \frac{\partial x_M}{\partial J_{N+1}} & \cdots & \frac{\partial x_M}{\partial J_{N+L}} \\ \hline \frac{\partial \mu_1}{\partial J_1} & \cdots & \frac{\partial \mu_1}{\partial J_N} & \frac{\partial \mu_1}{\partial J_{N+1}} & \cdots & \frac{\partial \mu_1}{\partial J_{N+L}} \\ \vdots & & \vdots & \vdots & & \vdots \\ \frac{\partial \mu_K}{\partial J_1} & \cdots & \frac{\partial \mu_K}{\partial J_N} & \frac{\partial \mu_K}{\partial J_{N+1}} & \cdots & \frac{\partial \mu_K}{\partial J_{N+L}} \end{array}\right). \tag{A3}$$

Equation (12) is generalized to

$$\boldsymbol{A}\tilde{\boldsymbol{S}} = -\left(\begin{array}{ccc|ccc} \frac{\partial r_1}{\partial k_1} & \cdots & 0 & & & \\ \vdots & \ddots & \vdots & & \boldsymbol{0} & \\ 0 & \cdots & \frac{\partial r_N}{\partial k_N} & & & \\ \hline & & & 1 & \cdots & 0 \\ & \boldsymbol{0} & & \vdots & \ddots & \vdots \\ & & & 0 & \cdots & 1 \end{array}\right), \tag{A4}$$

where $r_{j,m} \coloneqq \frac{\partial r_j}{\partial x_m}$. All partial derivatives are evaluated at the steady state.

With Eq. (4) in mind, Theorem 1 is generalized to Theorem 8.

Theorem 8. If $\boldsymbol{A}$ is invertible,

$$\tilde{\boldsymbol{S}} \propto -\boldsymbol{A}^{-1} \coloneqq \boldsymbol{A} \tag{A5}$$

Remark 5. (The selection of the cokernel basis). The values of $\frac{\partial x_m}{\partial k_n}$ are independent of the choice of bases for $\ker \boldsymbol{v}$ and $\ker \boldsymbol{v}^T$, which is proved in much the same way as Lemma 1. Hence, when our focus is solely on the effects of perturbations to the reaction rate parameters, we have the flexibility to choose the bases as we prefer. However, if our interest lies in the effects of perturbations to the conserved quantities, it is crucial to carefully select the basis for $\ker \boldsymbol{v}^\top$. If $\operatorname{supp}\boldsymbol{d}_a \subset \operatorname{supp}\boldsymbol{d}_b$ for some a, b $(1 \leqslant a \neq b \leqslant L)$, the perturbation of

d_a can affect d_b, in which case the partial derivative $\frac{\partial x_m}{\partial d_a}$ is difficult to interpret. To avoid choosing such a basis, it is recommended to find a basis by transforming $\boldsymbol{\nu}^\top$ into its reduced row-echelon form (RREF). When finding buffering structures, choosing the cokernel basis requires additional caution (see also Appendix A 4 b).

2. Buffering structure

We briefly review the law of localization and buffering structure [13].

Definition 5. (Generalized definition of a buffering structure). [13] A subnetwork $\Gamma = (\mathfrak{m}_\Gamma, \mathfrak{r}_\Gamma)$ ($\mathfrak{m}_\Gamma$, $\mathfrak{r}_\Gamma$ are subsets of chemicals and reactions, respectively) of a regular CRN is a buffering structure if it satisfies

(1) None of the reaction rates of the reactions in $\mathfrak{r}_\Gamma^c$ are dependent on the concentrations of chemicals within $\mathfrak{m}_\Gamma$, i.e., $\frac{\partial r_n}{\partial x_m}|_{\boldsymbol{x}} = 0$ at all $\boldsymbol{x}$, $\forall n \in \mathfrak{r}_\Gamma^c, \forall m \in \mathfrak{m}_\Gamma$, where $\mathfrak{r}_\Gamma^c$ means the complement of $\mathfrak{r}_\Gamma$ in all reactions in the CRN (output-complete).

(2) $\lambda(\Gamma) = 0$ with $\lambda(\Gamma) = -|\mathfrak{m}_\Gamma| + |\mathfrak{r}_\Gamma| - N(\mathfrak{r}_\Gamma) + N_c(\mathfrak{m}_\Gamma)$.

Here, $|\mathfrak{m}_\Gamma|$ and $|\mathfrak{r}_\Gamma|$ are the size of $\mathfrak{m}_\Gamma$ and $\mathfrak{r}_\Gamma$, respectively, $N(\mathfrak{r}_\Gamma)$ is the number of stoichiometric cycles in $\mathfrak{r}_\Gamma$. To be precise, $N(\mathfrak{r}_\Gamma) \coloneqq \dim \{\boldsymbol{x} \in \ker \boldsymbol{\nu} \mid \operatorname{supp} \boldsymbol{x} \subset \mathfrak{r}_\Gamma\}$, where $\operatorname{supp} \boldsymbol{r} \coloneqq \{i \mid x_i \neq 0\}$ for $\boldsymbol{r} \in \mathbb{R}^N$. $N_c(\mathfrak{m}_\Gamma)$ is the number of independent conserved quantities containing at least one element in $\mathfrak{m}_\Gamma$. To be precise, $N_c(\mathfrak{m}_\Gamma) \coloneqq \dim \{\boldsymbol{P}^{\mathfrak{m}_\Gamma} \boldsymbol{x} \mid \boldsymbol{x} \in \ker \boldsymbol{\nu}^\top\}$, where $\boldsymbol{P}^{\mathfrak{m}_\Gamma} \in \mathbb{R}^{M \times M}$ is a projection matrix onto the space associated with $\mathfrak{m}_\Gamma$ defined as

$$\boldsymbol{P}^{\mathfrak{m}_\Gamma}_{j,j'} = \delta_{j,j'} \text{ if } j, j' \in \mathfrak{m}_\Gamma. \text{ Otherwise } \boldsymbol{P}^{\mathfrak{m}_\Gamma}_{j,j'} = 0. \tag{A6}$$

Note that the definition of a buffering structure is indifferent to the choice of bases for $\ker \boldsymbol{\nu}$ or $\ker \boldsymbol{\nu}^\top$.

From Theorem 8 we can deduce Theorem 9.

Theorem 9. (Law of localization). [13] We consider a regular CRN with conserved quantities. We choose a basis for $\ker \boldsymbol{\nu}^\top$ as $\{\boldsymbol{d}_a\}_{a=1}^L$ in the following way. First, we start with the basis vectors for $\{\boldsymbol{x} \in \ker \boldsymbol{\nu}^\top \mid \operatorname{supp} \boldsymbol{x} \subset \mathfrak{m}_\Gamma^c\}$. Then, we repeatedly add a vector not in the span of the vectors to the set until it spans $\ker \boldsymbol{\nu}^\top$. If a subnetwork $\Gamma = (\mathfrak{m}_\Gamma, \mathfrak{r}_\Gamma)$ ($\mathfrak{m}_\Gamma$, $\mathfrak{r}_\Gamma$ are subsets of chemicals and reactions, respectively) is a buffering structure, then the following two hold.

(1) For any reaction $n \in \mathfrak{r}_\Gamma$ and for any chemical $m \in \mathfrak{m}_\Gamma^c$, $\frac{\partial x_m}{\partial k_n} = 0$ holds.

(2) For any a satisfying $\operatorname{supp} \boldsymbol{d}_a \cap \mathfrak{m}_\Gamma \neq \emptyset$ and for any chemical $m \in \mathfrak{m}_\Gamma^c$, $\frac{\partial x_m}{\partial d_a} = 0$ holds.

Theorem 9 states that the steady-state chemical concentrations outside of a buffering structure do not change under perturbations to reaction rate parameters or conserved quantities within the buffering structure. Since Γ is output-complete, the steady-state reaction fluxes outside of a buffering structure do not change under these perturbations either, as discussed in Remark 2.

3. The inverse theorem

We provide a generalized definition of a regulatory module.

Definition 6. (General definition of a regulatory module). In the case of a regular CRN with $\dim \ker \boldsymbol{\nu}^\top > 0$, we choose a basis of $\ker \boldsymbol{\nu}^\top$ as $\{\boldsymbol{d}_a\}_{a=1}^L$. We define a subnetwork $\Psi = (\mathfrak{m}_\Psi, \mathfrak{r}_\Psi)$ ($\mathfrak{m}_\Psi$, $\mathfrak{r}_\Psi$ represent subsets of chemicals and reactions, respectively) as a regulatory module under the cokernel basis $\{\boldsymbol{d}_a\}_{a=1}^L$ if it meets the following criteria:

(1) Ψ is output-complete.

(2a) For any reaction $n \in \mathfrak{r}_\Psi$ and any chemical $m \in \mathfrak{m}_\Psi^c$, $\frac{\partial x_m}{\partial k_n} = 0$.

(2b) For any a such that $\operatorname{supp} \boldsymbol{d}_a \cap \mathfrak{m}_\Psi \neq \emptyset$ and any chemical $m \in \mathfrak{m}_\Psi^c$, $\frac{\partial x_m}{\partial d_a} = 0$.

Note that the definition of a regulatory module depends on the choice of a basis of $\ker \boldsymbol{\nu}^\top$, whereas a buffering structure is defined independently of the choice.

According to the law of localization (Theorem 9), a buffering structure is a regulatory module for some choice of the basis for $\ker \boldsymbol{\nu}^\top$. It can be proved that the inverse theorem of the law of localization holds, which states that if a subnetwork is a regulatory module under some choice of the basis for $\ker \boldsymbol{\nu}^\top$, the subnetwork is a buffering structure.

Theorem 10. (Generalized inverse theorem of the law of localization). We consider a regular CRN. If $\dim \ker \boldsymbol{\nu}^\top > 0$, we choose a basis for $\ker \boldsymbol{\nu}^\top$ as $\{\boldsymbol{d}_a\}_{a=1}^L$. Let Ψ be a regulatory module under the cokernel basis $\{\boldsymbol{d}_a\}_{a=1}^L$. Then, Ψ is a buffering structure.

Proof of Theorem 10. The proof is almost the same as that of Theorem 3. Briefly, by appropriately choosing bases for $\ker \boldsymbol{\nu}$ and $\ker \boldsymbol{\nu}^T$ and the orderings of the indices of $\boldsymbol{A}$, $\boldsymbol{A}$ becomes a block matrix in which the lower left block is the zero matrix [Fig. 6 (left)]. Since $\boldsymbol{A}$ is invertible, the upper left block is horizontally long or square, i.e., $\lambda(\Psi) = -|\mathfrak{m}_\Psi| + |\mathfrak{r}_\Psi| - N(\mathfrak{r}_\Psi) + N_c(\mathfrak{m}_\Psi) \geqslant 0$. In addition, $\boldsymbol{S}$ becomes a block matrix in which the lower right block is the zero matrix, which can be proved in much the same way as the proof of Theorem 3 [Fig. 6 (right)]. Since $\boldsymbol{S}$ is invertible, the upper left block is horizontally long or square, i.e., $\lambda(\Psi) = -|\mathfrak{m}_\Psi| + |\mathfrak{r}_\Psi| - N(\mathfrak{r}_\Psi) + N_c(\mathfrak{m}_\Psi) \leqslant 0$. Thus, we obtain $\lambda(\Psi) = 0$. Since Ψ is output-complete, Ψ is a buffering structure. ■

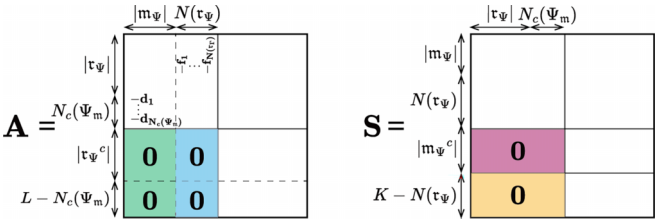

FIG. 6. Schematic depiction of $\boldsymbol{A}$ and $\boldsymbol{S}$ when $\Psi = (\mathfrak{m}_\Psi, \mathfrak{r}_\Psi)$ is a regulatory module. (Left) By collecting the indices associated with Ψ into the upper left corner, $\boldsymbol{A}$ can be a block matrix in which the lower left block is the zero matrix. (Right) $\boldsymbol{S}$ is also proved to a block matrix in which the lower left block is the zero matrix. See proof of Theorem 10.

From Theorem 9 and Theorem 10, we obtain the following theorem.

Theorem 11. (The equivalence between a buffering structure and a regulatory module). Let Ψ be the subnetwork of a regular CRN. The following are equivalent.

(i) Ψ is a buffering structure.

(ii) Ψ is a regulatory module for some choice of the basis for $\ker \boldsymbol{\nu}^\top$.

ALGORITHM 2. Finding all buffering structures.

Output: $\{Y_1, \ldots, Y_{L+N}\}$, where $Y_n = \{\mathfrak{m}_{Y_n}, \mathfrak{p}_{Y_n}\}$ ($\mathfrak{m}_{Y_n}$ is the set of chemicals and $\mathfrak{p}_{Y_n}$ is the set of parameters).
1: **for** $n = 1, \ldots, L+N$
2: $\quad \mathfrak{m}_{Y_n} \leftarrow \{\}$, $\mathfrak{p}_{Y_n} \leftarrow \{n\}$
3: $\quad \mathfrak{m}_{Y_n} \leftarrow \mathfrak{m}_{Y_n} \cup M(\mathfrak{p}_{Y_n})$
4: $\quad$ **if** $\mathfrak{p}_{Y_n} \supset R(\mathfrak{m}_{Y_n})$ and $\mathfrak{p}_{Y_n} \supset R_q(\mathfrak{m}_{Y_n})$ **then**
5: $\quad\quad Y_n \leftarrow \{\mathfrak{m}_{Y_n}, \mathfrak{p}_{Y_n}\}$
6: $\quad$ **else**
7: $\quad\quad \mathfrak{p}_{Y_n} \leftarrow \mathfrak{p}_{Y_n} \cup R(\mathfrak{m}_{Y_n}) \cup R_q(\mathfrak{m}_{Y_n})$
8: $\quad\quad$ **go to3**
9: $\quad$ **end if**
10: **end for**
11: **return** $\{Y_1, \ldots, Y_{N+L}\}$

4. The algorithm to find buffering structures

a. Algorithm

We generalize the algorithm to find buffering structures in CRNs with conserved quantities. Here, we describe the algorithm to find regulatory modules under the specific choice of the basis for $\ker \boldsymbol{\nu}^\top$, denoted by $\{\boldsymbol{d}_a\}_{a=1}^L$. How we should choose the basis is discussed in Appendix A 4 b. We define $\{J_1, \ldots, J_N, J_{N+1}, \ldots, J_{N+L}\} \coloneqq \{k_1, \ldots, k_N, d_1, \ldots, d_L\}$ as shown in Eq. (A1). For each reaction rate parameter or conserved quantity n ($1 \leqslant n \leqslant N+L$), we find the minimum buffering structure containing parameter n through the following procedures (Algorithm 2).

Similar to the notations in the main text, we introduce some notations. For each parameter n ($n = 1, \ldots, N+L$), which corresponds to either the reaction rate parameter or conserved quantity, we let $M(n)$ be the set of chemicals whose steady-state concentrations are affected by the perturbation to n. For a reaction set $\mathcal{N}$, we let $M(\mathcal{N}) \coloneqq \bigcup_{n\in\mathcal{N}} M(n)$. For a chemical m, we let $R(m)$ be the set of reactions whose reaction rates are dependent on m, i.e., $R(m) \coloneqq \{n \mid \frac{\partial r_n}{\partial x_m} \neq 0\}$. We also let $R_q(m)$ be the set of conserved quantities that contain m, i.e., $R_q(m) \coloneqq \{d_a \mid m \in \operatorname{supp} \boldsymbol{d}_a\}$. For a chemical set $\mathfrak{m}$, we let $R(\mathfrak{m}) \coloneqq \bigcup_{m\in\mathfrak{m}} R(m)$ and $R_q(\mathfrak{m}) \coloneqq \bigcup_{m\in\mathfrak{m}} R_q(m)$.

To obtain the minimum buffering structure that contains the parameter n, we begin by constructing a subnetwork that contains only parameter n. Then, we add $M(n)$ to the subnetwork. To make the subnetwork output-complete, we add $R(M(n))$ to the subnetwork. We also add $R_q(M(n))$ to the subnetwork. Again, we add chemicals that are influenced by the newly added parameters. The subnetwork can be made output-complete by adding some reactions. We also add conserved quantities that contain at least one of the newly added chemicals. We repeat this procedure until there are no reactions or conserved quantities to be added. The resulting subnetwork Y_n is output-complete and the effects of the perturbations to the reaction rate parameters or conserved quantities in Y_n are confined inside Y_n, indicating that Y_n is a regulatory module under the basis $\{\boldsymbol{d}_a\}_{a=1}^L$. According to Theorem 10, Y_n is a buffering structure. This procedure stops in a finite number of steps since the number of chemicals plus the number reactions in a network is finite.

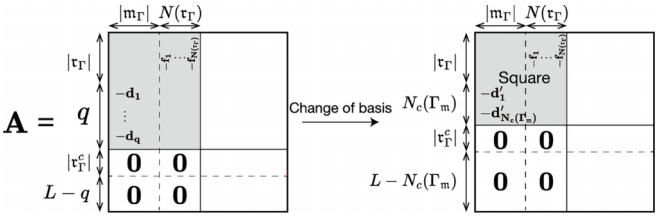

FIG. 7. Schematic depiction of the matrix $\boldsymbol{A}$ related to the proof of Proposition 2. (Left) By collecting the indices associated with Γ into the upper-left corner, the matrix $\boldsymbol{A}$ can be a block matrix in which the lower right is the zero matrix. (Right) After the change of basis from $\{\boldsymbol{d}_a\}_{a=1}^L$ to $\{\boldsymbol{d}'_a\}_{a=1}^L$, the matrix $\boldsymbol{A}$ will be a block diagonal matrix.

We iterate the procedure for $n = 1, \ldots, N+L$ and remove duplicates, obtaining $Y_{p_1}, \ldots, Y_{p_s}$ ($1 \leqslant p_1 < \ldots < p_s \leqslant N+L$).

b. Choice of the cokernel basis

Notably, to find all buffering structures, we have to find regulatory modules for all possible choices of the basis for $\ker \boldsymbol{\nu}^\top$, which is not feasible since there are infinitely many ways to select a basis. However, in most cases, finding regulatory modules under a single basis is sufficient (Proposition 2).

Proposition 2. We consider a regular CRN. Suppose that a basis $\{\boldsymbol{d}_a\}_{a=1}^L$ for $\ker \boldsymbol{\nu}^\top$ can be chosen such that

$$\operatorname{supp} \boldsymbol{d}_a \cap \operatorname{supp} \boldsymbol{d}_b = \emptyset \text{ for all } a, b \ (1 \leqslant a \neq b \leqslant L), \quad \text{(A7)}$$

i.e., no two conserved quantities share constituent chemicals. Then, finding regulatory modules under $\{\boldsymbol{d}_a\}_{a=1}^L$ is sufficient to identify all buffering structures.

Proof of Proposition 2. Suppose on the contrary that there exists a buffering structure $\Gamma = (\mathfrak{m}_\Gamma, \mathfrak{r}_\Gamma)$, which is not a regulatory module under the basis $\{\boldsymbol{d}_a\}_{a=1}^L$. If $\operatorname{supp} \boldsymbol{d}_a \cap \mathfrak{m}_\Gamma = \emptyset$ for all $a = 1, \ldots, L$, Γ is a regulatory module regardless of the choice of basis. Therefore, we assume, without loss of generality, that

$$\begin{aligned} &\operatorname{supp} \boldsymbol{d}_a \cap \mathfrak{m}_\Gamma \neq \emptyset, \quad \text{if } a = 1, \ldots, q, \\ &\operatorname{supp} \boldsymbol{d}_a \cap \mathfrak{m}_\Gamma = \emptyset, \quad \text{Otherwise,} \end{aligned} \quad \text{(A8)}$$

where q is the size of the set $\{\boldsymbol{d}_a \mid \operatorname{supp} \boldsymbol{d}_a \cap \mathfrak{m}_\Gamma \neq \emptyset\}$. Let $\tilde{\boldsymbol{d}}_a$ be the projection of $\boldsymbol{d}_a$ into $\mathfrak{m}_\Gamma$. Based on Eq. (A7), $\tilde{\boldsymbol{d}}_1, \ldots, \tilde{\boldsymbol{d}}_q$ are linearly independent.

We denote the basis of $\ker \boldsymbol{\nu}$ by $\{\boldsymbol{f}_1, \ldots, \boldsymbol{f}_{N(\mathfrak{r}_\Gamma)}, \boldsymbol{f}_{N(\mathfrak{r}_\Gamma+1)}, \ldots, \boldsymbol{f}_K\}$, as in Lemma 2. As demonstrated in the proof of Theorem 3, by arranging the orders of the column and row indices of $\boldsymbol{A}$, we can rewrite $\boldsymbol{A}$ into the block form as shown in Fig. 7 (left). The structure of block matrices in Fig. 7 (left) can be obtained by collecting the indices associated with Γ into the upper-left corner: The column indices at the upper left block consist of the chemicals in $\mathfrak{m}_\Gamma$ followed by $-\boldsymbol{f}_1, \ldots, -\boldsymbol{f}_{N(\mathfrak{r}_\Gamma)}$, which represent the basis vectors of $V_{\mathfrak{r}_\Gamma}$. The row indices consist of the reactions in $\mathfrak{r}_\Gamma$ and $-\boldsymbol{d}_1, \ldots, -\boldsymbol{d}_q$. The left block vanishes, similar to the proof of Theorem 3. Regularity of the system indicates $|\mathfrak{m}_\Gamma| + N(\mathfrak{r}_\Gamma) \leqslant |\mathfrak{r}_\Gamma| + q$. If $|\mathfrak{m}_\Gamma| + N(\mathfrak{r}_\Gamma) = |\mathfrak{r}_\Gamma| + q$, the sensitivity matrix $\boldsymbol{S} = -\boldsymbol{A}^{-1}$ is a block-diagonal matrix, which means that Γ is a regulatory module under the basis

$\{\boldsymbol{d}_a\}_{a=1}^{L}$. Because Γ is not a regulatory module under $\{\boldsymbol{d}_a\}_{a=1}^{L}$, we have

$$|\mathfrak{m}_\Gamma| + N(\mathfrak{r}_\Gamma) < |\mathfrak{r}_\Gamma| + q. \tag{A9}$$

There exists another basis for $\ker \boldsymbol{v}^\top$, denoted by $\{\boldsymbol{d}'_a\}_{a=1}^{L}$, such that $|\{\mathrm{supp}\,\boldsymbol{d}'_i \mid \boldsymbol{d}'_i \cap \mathfrak{m}_\Gamma \neq \emptyset\}| = N_c(\mathfrak{m}_\Gamma)$, as stated in Theorem 9. Since Γ is a buffering structure,

$$|\mathfrak{m}_\Gamma| + N(\mathfrak{r}_\Gamma) = |\mathfrak{r}_\Gamma| + N_c(\mathfrak{m}_\Gamma), \tag{A10}$$

and $\boldsymbol{A}$ becomes a block diagonal matrix [Fig. 7 (right)]. From Eqs. (A9) and (A10), we have $N_c(\mathfrak{m}_\Gamma) < q$. This means that a change of the basis from $\{\boldsymbol{d}_a\}_{a=1}^{L}$ to $\{\boldsymbol{d}'_a\}_{a=1}^{L}$ results in a reduction in the number of vectors that have at least one nonzero entry in $\mathfrak{m}_\Gamma$. Consequently, there exists i $(1 \leqslant i \leqslant L)$ such that $\boldsymbol{d}'_i = w_1\boldsymbol{d}_1 + \ldots + w_L\boldsymbol{d}_L$ (at least one of $w_1, \ldots, w_L$ is nonzero) and that $\mathrm{supp}\,\boldsymbol{d}'_i \cap \mathfrak{m}_\Gamma = \emptyset$. By projecting $\boldsymbol{d}'_i$ into $\mathfrak{m}_\Gamma$, we obtain $\boldsymbol{0} = w_1\tilde{\boldsymbol{d}}_1 + \ldots + w_q\tilde{\boldsymbol{d}}_q$. This contradicts the fact that $\tilde{\boldsymbol{d}}_1, \ldots, \tilde{\boldsymbol{d}}_q$ are linearly independent, thereby completing the proof. ■

In most CRNs, it is possible to choose the basis for $\ker \boldsymbol{v}^T$ in such a way that Eq. (A7) holds. In this case, finding regulatory modules under the single choice of basis is sufficient to find all buffering structures.

Example 5. We consider a pathway, shown in Fig. 8(a). We choose the basis for $\ker \boldsymbol{v}^T$ as $\boldsymbol{d}_1 = (1,1,0,0,0,0)^\top$, $\boldsymbol{d}_2 = (0,0,1,1,0,0)^\top$, $\boldsymbol{d}_3 = (0,0,0,0,1,1)^\top$, which satisfies Eq. (A7). The matrix $\mathbf{A}$ is

$$\mathbf{A} = \left(\begin{array}{cccccc|ccc}
r_{1,\mathrm{A}} & 0 & 0 & 0 & 0 & 0 & -1 & 0 & 0 \\
0 & r_{2,\mathrm{B}} & 0 & 0 & 0 & 0 & -1 & 0 & 0 \\
0 & r_{3,\mathrm{B}} & r_{3,\mathrm{C}} & 0 & 0 & 0 & 0 & -1 & 0 \\
0 & 0 & 0 & r_{4,\mathrm{D}} & 0 & 0 & 0 & -1 & 0 \\
0 & 0 & 0 & r_{5,\mathrm{D}} & r_{5,\mathrm{E}} & 0 & 0 & 0 & -1 \\
0 & 0 & 0 & 0 & 0 & r_{6,\mathrm{F}} & 0 & 0 & -1 \\
-1 & -1 & 0 & 0 & 0 & 0 & 0 & 0 & 0 \\
0 & 0 & -1 & -1 & 0 & 0 & 0 & 0 & 0 \\
0 & 0 & 0 & 0 & -1 & -1 & 0 & 0 & 0
\end{array}\right), \tag{A11}$$

and the sensitivities are determined as

$$\mathbf{S} = -\mathbf{A}^{-1} = \left(\begin{array}{ccccccccc}
* & * & 0 & 0 & 0 & 0 & * & 0 & 0 \\
* & * & 0 & 0 & 0 & 0 & * & 0 & 0 \\
* & * & * & * & 0 & 0 & * & * & 0 \\
* & * & * & * & 0 & 0 & * & * & 0 \\
* & * & * & * & * & * & * & * & * \\
* & * & * & * & * & * & * & * & * \\
\hline
* & * & 0 & 0 & 0 & 0 & * & 0 & 0 \\
* & * & * & * & 0 & 0 & * & * & 0 \\
* & * & * & * & * & * & * & * & *
\end{array}\right), \tag{A12}$$

where $*$ represents a nonzero response.

We obtain $M(1) = M(2) = \{\mathrm{A, B, C, D, E, F}\}$, $M(3) = M(4) = \{\mathrm{C, D, E, F}\}$, $M(5) = M(6) = \{\mathrm{E, F}\}$,

$M_q(d_1) = \{\mathrm{A, B, C, D, E, F}\}$, $M_q(d_2) = \{\mathrm{C, D, E, F}\}$, $M_q(d_3) = \{\mathrm{E,F}\}$.

We also obtain $R(\mathrm{A}) = \{1\}$, $R(\mathrm{B}) = \{2, 3\}$, $R(\mathrm{C}) = \{3\}$, $R(\mathrm{D}) = \{4, 5\}$, $R(\mathrm{E}) = \{5\}$, $R(\mathrm{F}) = \{6\}$,

$R_q(\mathrm{A}) = R_q(\mathrm{B}) = \{d_1\}$, $R_q(\mathrm{C}) = R_q(\mathrm{D}) = \{d_2\}$, $R_q(\mathrm{E}) = R_q(\mathrm{F}) = \{d_3\}$.

The minimum set of buffering structures are given by the Algorithm 2: $Y_1 = Y_2 = \{\{\mathrm{A, B, C, D, E, F}\}, \{1, 2, 3, 4, 5, 6, d_1, d_2, d_3\}\}$, $Y_3 = Y_4 = \{\{\mathrm{C, D, E, F}\}, \{3, 4, 5, 6, d_2, d_3\}\}$, $Y_5 = Y_6 = \{\{\mathrm{E, F}\}, \{5, 6, d_3\}\}$.

The construction of the hierarchy graph can be done in much the same way as the method described in the main text [Fig. 8(b)].

Remark 6. (Strategy for finding all buffering structures when there is no basis satisfying Eq. (A7)). In some CRNs, choosing a basis satisfying Eq. (A7) is impossible. Even in such cases, we may be able to find all buffering structures using the following strategy.

First, under the specific choice of basis $\{\boldsymbol{d}_a\}_{a=1}^{L}$ calculated from RREF, we find regulatory modules $\Psi_1, \ldots, \Psi_s$, which are buffering structures from Theorem 10. However, there can be another buffering structure Γ, because there can exist another choice of cokernel basis such that Γ is a regulatory module under the basis. To check this possibility, we examine whether each $\Psi_i = (\mathfrak{m}_{\Psi_i}, \mathfrak{r}_{\Psi_i})$ includes a smaller buffering structure (Because the intersection of two buffering structures is also a buffering structure, it is sufficient to check this for each Ψ_i). From the law of localization (Theorem 9), if Ψ_i includes a hidden buffering structure Γ, perturbations to reaction rate parameters in Γ do not affect the steady-state concentration of chemicals in $\Psi_i \setminus \Gamma$. In other words, if some reaction $n \in \mathfrak{r}_{\Psi_i}$ does not affect some chemical $m \in \mathfrak{m}_{\Psi_i}$, and the nonzero response is not explained by the identified buffering structure $\Psi_1, \ldots, \Psi_s$, there is a possibility that Ψ_i is decomposed into smaller buffering structures. In such cases, changing the basis among $\{\boldsymbol{d}_a \mid \mathrm{supp}\,\boldsymbol{d}_a \cap \mathfrak{m}_{\Psi_i} \neq \emptyset\}$ is recommended as it will lead to find the hidden buffering structures.

APPENDIX B: THE LIST OF REACTIONS FOR E. COLI CENTRAL METABOLISM

(1) Glucose + PEP → G6P + PYR
(2) G6P → F6P
(3) F6P → G6P
(4) F6P → F1,6P
(5) F1,6P → G3P + DHAP
(6) DHAP → G3P
(7) G3P → 3PG
(8) 3PG → PEP
(9) PEP → 3PG
(10) PEP → PYR

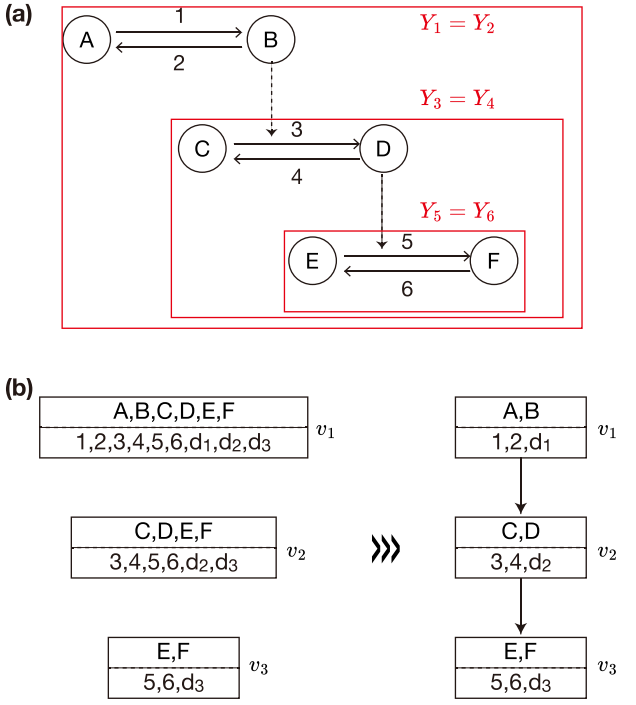

FIG. 8. Analysis for a hypothetical network with conserved quantities (Example 5). (a) Graphical representation of a CRN comprising six chemicals (A, B, C, D, E, F) and six reactions (1, 2, 3, 4, 5, 6) with three conserved quantities ($d_1 : x_A + x_B$, $d_2 : x_C + x_D$, and $d_3 : x_E + x_F$). Solid lines indicate chemical reactions, while the dashed line indicates active regulation. Each subnetwork enclosed by a red box (Y_i) is a buffering structure containing the reaction i. (b) The construction of the hierarchy graph. First, we construct a graph such that each Y_i is assigned to each node v_i. Then, we construct the hierarchy graph such that modulating the enzyme activity of reactions within a square box leads to nonzero responses in the chemicals within that box and those in the lower boxes, leaving the other chemicals unaffected.

(11) PYR → PEP
(12) PYR → AcCoA + CO2
(13) G6P → 6PG
(14) 6PG → Ru5P + CO2
(15) Ru5P → X5P
(16) Ru5P → R5P
(17) X5P + R5P → G3P + S7P
(18) G3P + S7P → X5P + R5P
(19) G3P + S7P → F6P + E4P
(20) F6P + E4P → G3P + S7P
(21) X5P + E4P → F6P + G3P
(22) F6P + G3P → X5P + E4P
(23) AcCoA + → CIT
(24) CIT → ICT
(25) ICT → 2−KG + CO2
(26) 2-KG → SUC + CO2
(27) SUC → FUM
(28) FUM → MAL
(29) MAL → OAA
(30) OAA → MAL
(31) PEP + CO2 → OAA
(32) OAA → PEP + CO2
(33) MAL → PYR + CO2
(34) ICT → SUC + Glyoxylate
(35) Glyoxylate + AcCoA → MAL
(36) 6PG → G3P + PYR
(37) AcCoA → Acetate
(38) PYR → Lactate
(39) AcCoA → Ethanol
(40) R5P → (output)
(41) OAA → (output)
(42) CO2 → (output)
(43) (input) → Glucose
(44) Acetate → (output)
(45) Lactate → (output)
(46) Ethanol → (output).

[1] Q. Wang, Y. Zhang, C. Yang, H. Xiong, Y. Lin, J. Yao, H. Li, L. Xie, W. Zhao, Y. Yao *et al.*, Acetylation of metabolic enzymes coordinates carbon source utilization and metabolic flux, Science **327**, 1004 (2010).

[2] R. A. Cairns, I. S. Harris, and T. W. Mak, Regulation of cancer cell metabolism, Nat. Rev. Cancer **11**, 85 (2011).

[3] Z. Li and H. Zhang, Reprogramming of glucose, fatty acid and amino acid metabolism for cancer progression, Cell. Mol. Life Sci. **73**, 377 (2016).

[4] N. Ishii, K. Nakahigashi, T. Baba, M. Robert, T. Soga, A. Kanai, T. Hirasawa, M. Naba, K. Hirai, A. Hoque *et al.*, Multiple high-throughput analyses monitor the response of *E. coli* to perturbations, Science **316**, 593 (2007).

[5] M. Miyo, M. Konno, N. Nishida, T. Sueda, K. Noguchi, H. Matsui, H. Colvin, K. Kawamoto, J. Koseki, N. Haraguchi *et al.*, Metabolic adaptation to nutritional stress in human colorectal cancer, Sci. Rep. **6**, 38415 (2016).

[6] S. Ohno, L.-E. Quek, J. R. Krycer, K. Yugi, A. Hirayama, S. Ikeda, F. Shoji, K. Suzuki, T. Soga, D. E. James *et al.*, Kinetic trans-omic analysis reveals key regulatory mechanisms for insulin-regulated glucose metabolism in adipocytes, iScience **23**, 101479 (2020).

[7] S. Drapela, D. Ilter, and A. P. Gomes, Metabolic reprogramming: A bridge between aging and tumorigenesis, Mol. Oncol. **16**, 3295 (2022).

[8] M. D. Rosenthal and R. H. Glew, *Medical Biochemistry: Human Metabolism in Health and Disease* (John Wiley & Sons, Hoboken, NJ, 2011).

[9] K. J. Kauffman, P. Prakash, and J. S. Edwards, Advances in flux balance analysis, Curr. Opin. Biotechnol. **14**, 491 (2003).

[10] J. D. Orth, I. Thiele, and B. Ø. Palsson, What is flux balance analysis? Nat. Biotechnol. **28**, 245 (2010).

[11] C. Ramon and J. Stelling, Functional comparison of metabolic networks across species, Nat. Commun. **14**, 1699 (2023).

[12] T. Okada and A. Mochizuki, Law of localization in chemical reaction networks, Phys. Rev. Lett. **117**, 048101 (2016).

[13] T. Okada and A. Mochizuki, Sensitivity and network topology in chemical reaction systems, Phys. Rev. E **96**, 022322 (2017).

[14] A. Mochizuki and B. Fiedler, Sensitivity of chemical reaction networks: a structural approach. 1. Examples and

the carbon metabolic network, J. Theor. Biol. **367**, 189 (2015).
[15] X. Y. Ni, T. Drengstig, and P. Ruoff, The control of the controller: molecular mechanisms for robust perfect adaptation and temperature compensation, Biophys. J. **97**, 1244 (2009).
[16] R. Steuer, S. Waldherr, V. Sourjik, and M. Kollmann, Robust signal processing in living cells, PLoS Comput. Biol. **7**, e1002218 (2011).
[17] T. Drengstig, I. Jolma, X. Ni, K. Thorsen, X. Xu, and P. Ruoff, A basic set of homeostatic controller motifs, Biophys. J. **103**, 2000 (2012).
[18] M. H. Khammash, Perfect adaptation in biology, Cell Systems **12**, 509 (2021).
[19] U. Alon, M. G. Surette, N. Barkai, and S. Leibler, Robustness in bacterial chemotaxis, Nature (London) **397**, 168 (1999).
[20] B. A. Mello and Y. Tu, Perfect and near-perfect adaptation in a model of bacterial chemotaxis, Biophys. J. **84**, 2943 (2003).
[21] U. Alon, *An Introduction to Systems Biology: Design Principles of Biological Circuits* (CRC Press, Boca Raton, FL, 2019).
[22] Y. Hirono, A. Gupta, and M. Khammash, Complete characterization of robust perfect adaptation in biochemical reaction networks, arXiv:2307.07444.
[23] A. Ferjani, K. Kawade, M. Asaoka, A. Oikawa, T. Okada, A. Mochizuki, M. Maeshima, M. Y. Hirai, K. Saito, and H. Tsukaya, Pyrophosphate inhibits gluconeogenesis by restricting UDP-glucose formation in vivo, Sci. Rep. **8**, 14696 (2018).
[24] E. Ravasz, A. L. Somera, D. A. Mongru, Z. N. Oltvai, and A.-L. Barabási, Hierarchical organization of modularity in metabolic networks, Science **297**, 1551 (2002).
[25] E. Segal, M. Shapira, A. Regev, D. Pe'er, D. Botstein, D. Koller, and N. Friedman, Module networks: identifying regulatory modules and their condition-specific regulators from gene expression data, Nat. Genet. **34**, 166 (2003).
[26] Q. Song, R. Grene, L. S. Heath, and S. Li, Identification of regulatory modules in genome scale transcription regulatory networks, BMC Syst. Biol. **11**, 140 (2017).
[27] S. Vlaic, T. Conrad, C. Tokarski-Schnelle, M. Gustafsson, U. Dahmen, R. Guthke, and S. Schuster, Moduledискoverer: Identification of regulatory modules in protein-protein interaction networks, Sci. Rep. **8**, 433 (2018).
[28] F. Horn, Necessary and sufficient conditions for complex balancing in chemical kinetics, Arch. Ration. Mech. Anal. **49**, 172 (1972).
[29] E. D. Sontag, Structure and stability of certain chemical networks and applications to the kinetic proofreading model of T-cell receptor signal transduction, IEEE Trans. Autom. Control **46**, 1028 (2001).
[30] M. Feinberg, The existence and uniqueness of steady states for a class of chemical reaction networks, Arch. Ration. Mech. Anal. **132**, 311 (1995).
[31] G. Craciun and M. Feinberg, Multiple equilibria in complex chemical reaction networks: II. The species-reaction graph, SIAM J. Appl. Math. **66**, 1321 (2006).
[32] M. Feinberg, *Foundations of Chemical Reaction Network Theory* (Springer, New York, 2019).
[33] Y. Hirono, T. Okada, H. Miyazaki, and Y. Hidaka, Structural reduction of chemical reaction networks based on topology, Phys. Rev. Res. **3**, 043123 (2021).
[34] B. Brehm and B. Fiedler, Sensitivity of chemical reaction networks: A structural approach. 3. Regular multimolecular systems, Math. Methods Appl. Sci. **41**, 1344 (2018).
[35] T. Okada, J.-C. Tsai, and A. Mochizuki, Structural bifurcation analysis in chemical reaction networks, Phys. Rev. E **98**, 012417 (2018).
[36] T. Okada, A. Mochizuki, M. Furuta, and J.-C. Tsai, Flux-augmented bifurcation analysis in chemical reaction network systems, Phys. Rev. E **103**, 062212 (2021).
[37] H. Ogata, S. Goto, K. Sato, W. Fujibuchi, H. Bono, and M. Kanehisa, Kegg: Kyoto encyclopedia of genes and genomes, Nucleic Acids Res. **27**, 29 (1999).
[38] H. Jeong, B. Tombor, R. Albert, Z. N. Oltvai, and A.-L. Barabási, The large-scale organization of metabolic networks, Nature (London) **407**, 651 (2000).
[39] G. Joshi-Tope, M. Gillespie, I. Vastrik, P. D'Eustachio, E. Schmidt, B. de Bono, B. Jassal, G. Gopinath, G. Wu, L. Matthews *et al.*, Reactome: A knowledgebase of biological pathways, Nucleic Acids Res. **33**, D428 (2005).
[40] P. D. Karp, C. A. Ouzounis, C. Moore-Kochlacs, L. Goldovsky, P. Kaipa, D. Ahrén, S. Tsoka, N. Darzentas, V. Kunin, and N. López-Bigas, Expansion of the biocyc collection of pathway/genome databases to 160 genomes, Nucleic Acids Res. **33**, 6083 (2005).
[41] N. C. Duarte, S. A. Becker, N. Jamshidi, I. Thiele, M. L. Mo, T. D. Vo, R. Srivas, and B. Ø. Palsson, Global reconstruction of the human metabolic network based on genomic and bibliomic data, Proc. Natl. Acad. Sci. USA **104**, 1777 (2007).
[42] R. Caspi, R. Billington, L. Ferrer, H. Foerster, C. A. Fulcher, I. M. Keseler, A. Kothari, M. Krummenacker, M. Latendresse, L. A. Mueller *et al.*, The metacyc database of metabolic pathways and enzymes and the biocyc collection of pathway/genome databases, Nucleic Acids Res. **44**, D471 (2016).
[43] W. Ma, A. Trusina, H. El-Samad, W. A. Lim, and C. Tang, Defining network topologies that can achieve biochemical adaptation, Cell **138**, 760 (2009).
[44] J. Shen, F. Liu, Y. Tu, and C. Tang, Finding gene network topologies for given biological function with recurrent neural network, Nat. Commun. **12**, 3125 (2021).
[45] T. Frei, C.-H. Chang, M. Filo, A. Arampatzis, and M. Khammash, A genetic mammalian proportional–integral feedback control circuit for robust and precise gene regulation, Proc. Natl. Acad. Sci. USA **119**, e2122132119 (2022).
[46] M. Filo, S. Kumar, and M. Khammash, A hierarchy of biomolecular proportional-integral-derivative feedback controllers for robust perfect adaptation and dynamic performance, Nat. Commun. **13**, 2119 (2022).
[47] A. Hishida, T. Okada, and A. Mochizuki, Patterns of change in regulatory modules of chemical reaction systems induced by network modification, PNAS Nexus **3**, pgad441 (2023).
[48] https://github.com/hishidagit/SSApy.